University of Colorado, Boulder
CU Scholar

Aerospace Engineering Sciences Graduate Theses & Dissertations

Aerospace Engineering Sciences

Spring 1-1-2011

G-Hardening of Commercial off the Shelf Components for Small Guided Projectiles

Jake John Decoto
University of Colorado at Boulder, decotoj@gmail.com

Follow this and additional works at: https://scholar.colorado.edu/asen_gradetds

Part of the Aerospace Engineering Commons, and the Mechanical Engineering Commons

G-HARDENING OF COMMERCIAL OFF THE SHELF COMPONENTS FOR

SMALL GUIDED PROJECTILES

by

JAKE DECOTO

B.S. Aerospace Engineering, University of Washington, 2006

A thesis submitted to the

Faculty of the Graduate School of the

University of Colorado in partial fulfillment

of the requirements for the degree of

Master of Science

Department of Aerospace Engineering Sciences

2011

This thesis entitled:
G-Hardening of Commercial off the Shelf Components for Small Guided Projectiles
written by Jake Decoto
has been approved for the Department of Aerospace Engineering Sciences

Prof. George Born

Prof. Robert Culp

Prof. Robert Leben

Date

The final copy of this thesis has been examined by the signatories, and we
Find that both the content and the form meet acceptable presentation standards
Of scholarly work in the above mentioned discipline.

Decoto, J. J. (M.S., Aerospace Engineering Sciences)

G-Hardening of Commercial off the Shelf Components for Small Guided Projectiles

Thesis directed by Prof. George Born

There is an increasing need for g-hardened electronic and electro-mechanical components to satisfy the needs of a growing array of guided projectile programs. Techniques such as encapsulation, underfilling and load path management have been used by the Army Research Labs to develop survivable components for artillery rounds that are subjected to up to 30,000 g's (1). However, g-hardening of the components necessary to enable the next generation of small caliber guided projectiles that could experience loads in the vicinity of 65,000 g's is a problem that is only starting to be addressed. This research aims to identify affordable Commercial Off The Shelf (COTS) components of interest to small caliber guided projectiles, and through experiment develop load path management techniques to allow their survivability in environments previously not possible.

Acknowledgements

The author would like to acknowledge Dr. George Born , Dr. Robert Culp, and Dr. Robert Leben for their open minds and for the time they gave in order to help a student they previously barely knew pursue his academic interests.

The author would also like to acknowledge Allison Curtin for her support throughout the project and her instrumental help as a quality control engineer, cardboard cutter, ballistics test technician, projectile finder, killer of mosquitoes, and crucial second set of eyes.

CONTENTS

Chapter

Tables

Table

Figures

Figure

CHAPTER 1

1 Introduction

1.1 Motivation

Ballistic guided projectiles have been in the U.S. military's arsenal for over a decade.
Most notable of which is the 155mm laser designated M712 Copperhead artillery round
employed with great effect in the 2003 conflict in Iraq. A follow on GPS guided 155mm
round, the M982 Excalibur shown in Figure 1, is now also beginning to be deployed.
The accuracy of such rounds at ranges of tens of kilometers is measured in centimeters.
This capability greatly increases effect on target while at the same time minimizing
collateral damage.

Figure 1: M982 Excalibur GPS guided 155mm round

Until very recently guided projectile development was limited to the 155mm artillery rounds and a few other large caliber systems. More recent efforts such as the DARPA SCORPION program have looked at in flight trajectory change capable rifle launched 40mm grenades, however these rounds are traveling at relatively low velocities and have limited guidance and control. The current DARPA EXACTO program is one of the first major development efforts whose goal is to bring the benefits of smart rounds to small arms, starting with the .50 BMG rounds used by snipers, Figure 2. A key technical challenge of any small caliber guided projectile program is that the components necessary for implementing guidance and achieving mid flight course corrections must be packaged in an extremely limited internal volume and withstand peak launch loads in the range of 40,000 to 65,000 g's in order to function in flight. These loads are higher than in larger caliber rounds and present a significant design challenge.

Figure 2: M107 sniper rifle and .50 (12.7mm) BMG round

Identifying or developing actuators, power sources, sensors, and other electronic components of the necessary form factor that can withstand gun launch loads is a central challenge to development of guided small caliber rounds. Also due to the relatively large number of small caliber rounds needed as compared to artillery rounds, and the one time use nature of projectiles, affordability is a key driver. In order to manage per round cost it is highly desirable to use COTS components whenever possible, as it is in any project. The behavior of such components, which in all but a few cases were never designed for these environments, under extreme g-loading is often unpredictable and highly dependent on the method of mounting in the interior cavity of the projectile. Experimental work to further examine the survivability of basic components is the focus of this project.

1.1 Scope and Outline

The goal of this work is to identify COTS components of potential interest to guided projectiles and to experimentally demonstrate g-hardening techniques to enable survival in relevant launch environments. Many components were considered for potential g-hardening including magnetometers, accelerometers, electric motors, processors, solenoid actuators, and batteries, among others. The factors used in selecting components for these experiments included potential benefit, cost, form factor, and degree to which past efforts may have g-hardened similar components in the past. This evaluation is described in detail in Section 3.3.3.

It was determined that electric motors present the best opportunity for this project. Electric motors have potential applications in guided projectiles as mechanical actuators in a wide range of control schemes several of which are described by Massey [16]. There are a number of motors available commercially for less than a dollar and potentially even

less if ordered in quantity. The motors identified were made for use as vibration motors in cell phones and pagers and as propulsion for very small radio controlled aircraft. Several different types of motors with the correct form factor for .50 class projectiles have been identified. These motors have been hardened to withstand drops from heights of a few feet where accelerations of up to 4,000 g's [1] can be seen, but have not been hardened to anywhere near the levels necessary for survival of gun launch loads. Similarly, components that may have been hardened for missile boost phase loads typically only require g-hardening in the range of 1200 g's [13]. Very little work has been published describing any applications where a small electric motor was successfully g-hardened for launch loads. The WASP gun launched UAV developed by MIT and Draper Laboratories [12] [15] is the only public domain application found where an electric motor was demonstrated in a high-G environment. For the 155mm projectile launched WASP the loads were up to 16,000 g's, much less than in a .50 projectile. In a paper dated 2001 describing development of a conceptual hypersonic projectile, Edwards states that "conventional aerodynamic control surfaces, together with the associated actuator mechanisms would be impractical for vehicles undergoing the very high accelerations associated with gun launch" [8]. The g-hardening of small electric motors would address the actuator mechanism of that problem.

This project developed an experimental means of launching rounds containing small electric motors in an environment relevant to the intended application and recovering those rounds for later analysis. Different methods of managing the load path were explored including encapsulation, mounting orientation, mass reduction and pre-loading. Five different types of motors were evaluated with a total of 40 launches performed to

explore the limits of g-hardening of these components. Peak launch loads achieved were as much as 57,000 G's.

CHAPTER 2

2 Background

2.1 Literature Survey of Selected Past Efforts in G-Hardening

Over the last several decades a number of efforts have been undertaken to g-harden various components for use in guided projectiles. While in the past efforts have typically been focused on 155mm class rounds, recent advances in miniaturization, in part due to the personal electronics industry, have made possible new classes of small caliber smart rounds. Small caliber is defined here as .50 (12.7mm) or smaller.

As objects get smaller and have reduced mass the forces experienced as a result of extreme acceleration environments will of course be less. This might suggest that the problem of g-hardening would become easier with the move to smaller calibers. However, smaller rounds such as the .50 BMG experience much higher peak g-loads than 155mm class artillery rounds and similar systems and therefore present challenges inherently different than the larger rounds. Figure 3 shows a measured in-bore acceleration profile for a modified M830A1 120mm antitank round. The peak g's in this case are just over 30,000 g's. However, a .50 BMG round will experience in the neighborhood of 65,000 g's. Intuitively this makes sense as the M830A1 achieves a muzzle velocity of 1400 m/s while the .50 BMG attains a muzzle velocity of 1220 m/s. This is only 13% less but the .50 BMG achieves this velocity over a barrel length much shorter. For the M830A1 when shot from an M1 Abrams tank barrel the acceleration occurs within a barrel length of 209 inches. The .50 BMG fired from an M107 rifle accelerates over a length of only 30 inches.
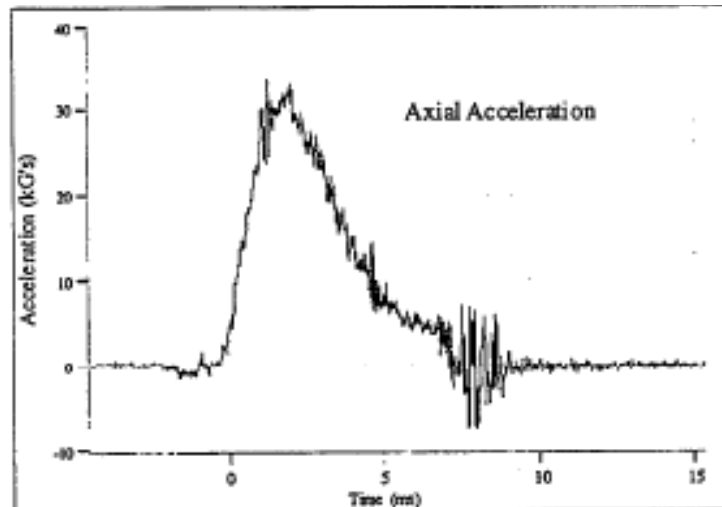
Figure 3: In bore acceleration profile for modified M830A1 120 mm High Explosive Antitank Projectile flight test [5]

While it has been demonstrated that the launch induced shock environment experienced by small projectiles of .50 or less is much different than their larger smart projectile counterparts, there has nevertheless been much work done in the larger caliber realm that is of great interest. The following sections attempt to highlight some of the more interesting public domain projects under which various components have been g-hardened for gun launch environments. Only efforts which have demonstrated published live fire results are included in this survey. This requirement precludes current research efforts, such as the 50-caliber (12.7mm) EXACTO program, which have not published live fire test results.

2.1.1 HSTSS Program

In order to support guided projectile development, the Army Research Lab's (ARL) Hardened Subminiature Telemetry and Sensor System (HSTSS) program developed a g-hardened telemetry package to instrument gun launched projectiles [4] [5] [6][20]. This effort demonstrated a high-g capable telemetry package to instrument 105mm class and

larger rounds with transmitters, data recorders, batteries, pressure transducers, spin sensors, accelerometers, yaw sensors and sun sensors.

2.1.2 WASP Experimental Gun Launched UAV

The Wide Area Surveillance Projectile (WASP) program [13], is a folded UAV design by the Massachusetts Institute of Technology (MIT) and Draper Labs that is deployed as a payload from a standard M-483A 155mm artillery cartridge. The program was started in 1997. As of published results dated 2002 one high-g test launch had occurred of a prototype meant to demonstrate packaging and flight performance [12] [15]. The WASP vehicle is designed for axial loads of up to 16,000 g's, much less than would be experienced in a small caliber round. The WASP design uses a brushless DC motor for propulsion.

2.1.3 SADARM Projectile

The US Army Sense and Destroy Armor (SADARM) projectile is a 155mm round that carries deployable sub-munitions capable of sensing and attacking enemy vehicles. The SADARM was the first fire-and-forget bullet employed by the Army and was first used in the 2003 invasion of Iraq. During launch the electronic components of the sub-munitions are subjected to loads of 15,000 g's [21]. Components of the sub-munitions are shown in Figure 7 and include an antenna, magnetometer and battery that have been packaged and g-hardened for that environment.
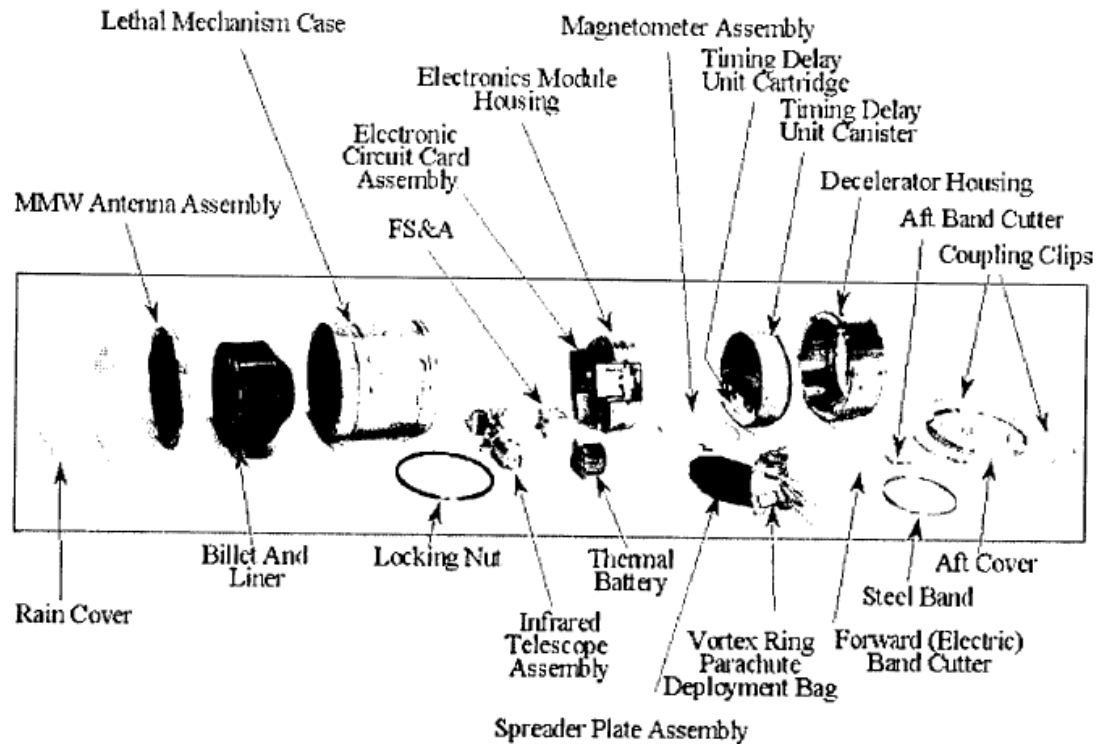
Figure 4: SADARM sub-munition components [21]

2.1.4 XM982 Excalibur Projectile

The XM982 Excalibur is a 155mm GPS guided artillery round currently in use by the US Army in both Iraq and Afghanistan. Excalibur represents the latest in large caliber smart rounds and its accuracy over ranges of tens of kilometers is measured in centimeters. In addition to increased accuracy, the ability to guide to a target and control its trajectory via fins allows Excalibur to increase range over conventional artillery rounds by using aerodynamic lift to fly a non-ballistic trajectory.

As part of the development process for Excalibur, Davis [7] describes experiments in which COTS magnetometers, accelerometers, and temperature sensors were shock tested under artillery round representative loads. The accelerometers used were Analog Devices ADXL250, ADXL78 and ADXL278, as well as the Silicon Designs SD1210.

Magnetometers tested were the Honeywell HMC1023. The temperature sensors were the Analog Devices AD22100SR. For these tests a shock table was used that exposed the components to up to 32,000 g's. Survivability varied by component and mounting method. The results were used to develop the DFuze inertial sensor suite which was used by both Excalibur and the Navy's Extended Range Guided Munition (ERGM) programs and based on non ballistic lab tests. The package is believed to be survivable to 30,000 g's [7].

2.1.5 M712 Copperhead Projectile

The M712 was the world's first smart munition. The copperhead round is a cannon launched 155mm round that guides itself via an optical seeker to a laser designated target. The copperhead was introduced in combat during the first Gulf War. The loads seen by the Copperhead round during gun launch are similar to that of EXCALIBUR and other 155mm smart rounds.

2.2 Other Extreme Acceleration Environments

Other extreme acceleration environments that could benefit from work to g-harden components for gun launch environments include explosives testing, rail launched orbital payloads [10], and instrumentation for destructive testing of materials such as armor.

2.3 Methods of G-Hardening Components

Berman [1] categorizes g-hardening techniques for electronic components into four categories: encapsulation, underfill, load path management, and component selection. Encapsulation, underfill and load path management techniques all seek to control the loads to which the component is subjected to. Component selection seeks to identify

components that can survive the loads. For the electromagnetic components being tested in this work these same techniques apply. However, they are employed in a somewhat different manner than they would be for electronic components, such as processors, accelerometers, and magnetometers, which are more typical subjects of published efforts in g-hardening for gun launch loads.

Encapsulation aims to fill up the space surrounding the component and prevent its physical expansion under load into that space which might cause component failure. This is accomplished by inserting the component into the partially hollow projectile and then filling the space with a potting material. A wide variety of potting materials can be used. It is usually desirable that the potting materials be a liquid that can flow into small crevices where it would then harden. One compound used at the Army Research Labs [1] for potting electronics is Stycast 1090 which is a hard drying foaming material. Other materials used are described by Quesenberry [17] . Once set the potting material provides a rigid structural support to the encased components. In addition to providing structural support potting materials can also provide some dampening. For this work it was desired to find a rigid setting potting material that was effective and very inexpensive. This ruled out obtaining Stycast 1090 which can only be bought in large quantities and is relatively expensive. A number of epoxies and commercial foams were tried. However with these it was very difficult to remove the component post launch and recovery for analysis. Finally, it was found that wax provides an effective structural support while also allowing for easy removal of the component when heat is applied.   Section 3.4 describes the encapsulation of components for this project in detail.

Underfill, as described in Berman [1], is a method of using epoxy to fill the area surrounding solder joints in flip chip or ball grid array packages or in the case of chip scale packages (CSPs) between the CSP and the printed wiring board. This type of technique of course would not directly apply to g-hardening of small electric motors which is the primary focus of this effort. It is necessary to have some space inside the interior volume of the motors to enable free spinning of the axle and windings. However, it might be possible to fill some of the interior motor cavity if done carefully.

Load path management is any method which seeks to protect the component by isolating it from the acceleration induced loads. This could include design of an outer case, pre-loading part in either compression or tension, or any number of other techniques. In the case of this project a number of methods of mounting in rigid attachment points at various locations, as well as loading in compression, were investigated. These are described in detail in Section 3.4.

Careful component selection is also necessary for survival of high-g loads. Especially with mass produced COTS components there are often a wide variety of components that perform essentially the same function that may have drastically different characteristics under launch loads. Furthermore, it is possible that individual lots or batches of the same component may have drastically different characteristics as well. For this project a total of five different types of small electric motor were tested, procurement batches were also tracked in case of differences.

CHAPTER 3

3 Experimental Setup

3.1 Experimental Setup Outline

In order to accurately assess the survivability of small components under extreme high-g loads a test setup was constructed capable of launching components at speeds in excess of 2500 ft/s, and subsequently decelerating and recovering them. This setup is meant to accurately re-create the environment that would be experienced by a small guided projectile containing various electrical and electromechanical components that must be launched from a gun and then operate during the flight of that projectile. In order to isolate the cause of any component physical damage, it is important that the deceleration of the component be less violent than the initial acceleration. The basic components of the experimental setup are a soft capture device, cargo rounds, test components, launcher, ballistics chronograph, component physical and electrical characterization setup, and static loads test setup. The function of each experimental setup component can be summarized as follows:

- Soft Capture Device: Catches the launched projectile and decelerates it allowing recovering of the component.

- Cargo Round Projectiles: Allows packaging of test components within its internal volume for launching and is designed to be reusable if recovered in a soft capture device.

- Test Components: A series of small electric motors made for various low-g commercial applications.

- Launcher: Muzzleloading rifle for launching of cargo round projectiles using Pyrodex smokeless powder propellant.

- Ballistics Chronograph: Allows estimation of peak acceleration on launch by measuring the velocity of projectile at 10 to 15 feet from the muzzle.

- Component Physical/Electrical Characterization Setup: Allows for pre and post launch measuring of component physical and electrical characteristics to assess any changes and help analytically characterize forces experienced.
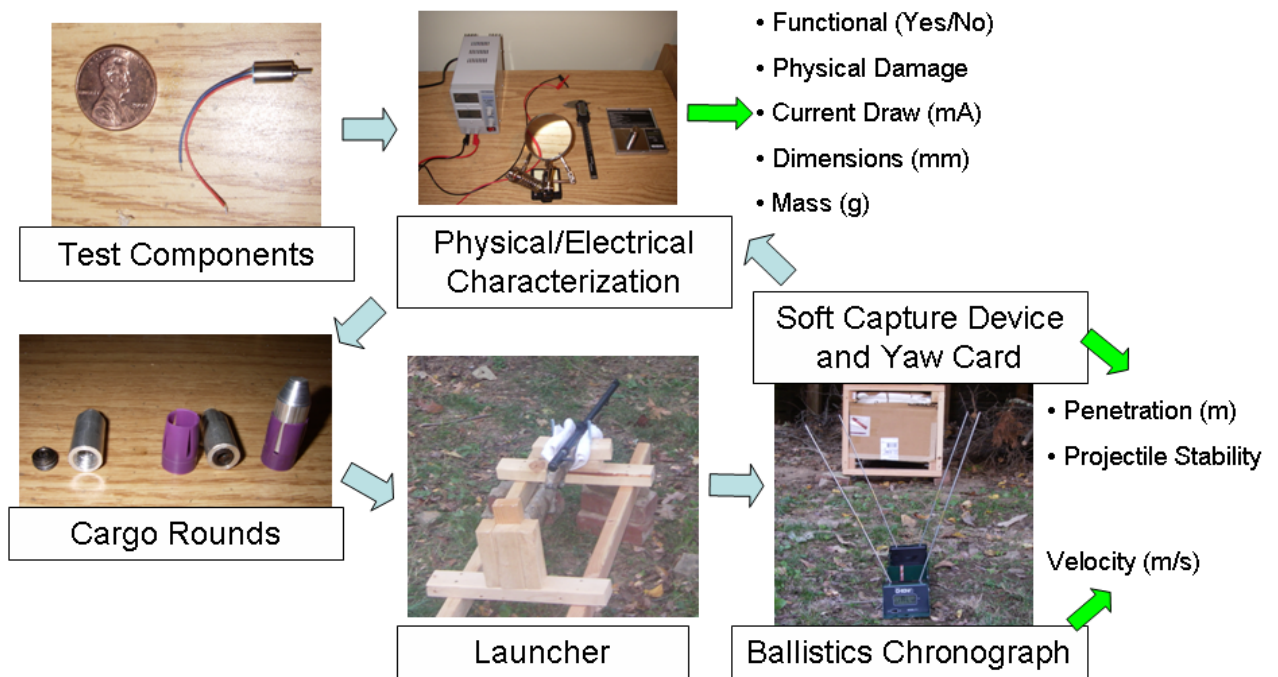
Figure 5: Experimental setup functional diagram

3.2 Test Plan

A series of test launches are required both to design the experimental setup and to iteratively determine the acceleration limit of components and then extend that limit. The variables for each component test will be the component type, modification to the component, how it is mounted, the cargo round used, powder load used, and deceleration material. Figure 6 shows a summary of the live fire tests required to validate the experimental setup. Once the experimental setup is validated iterative g-hardening development tests of components can begin.
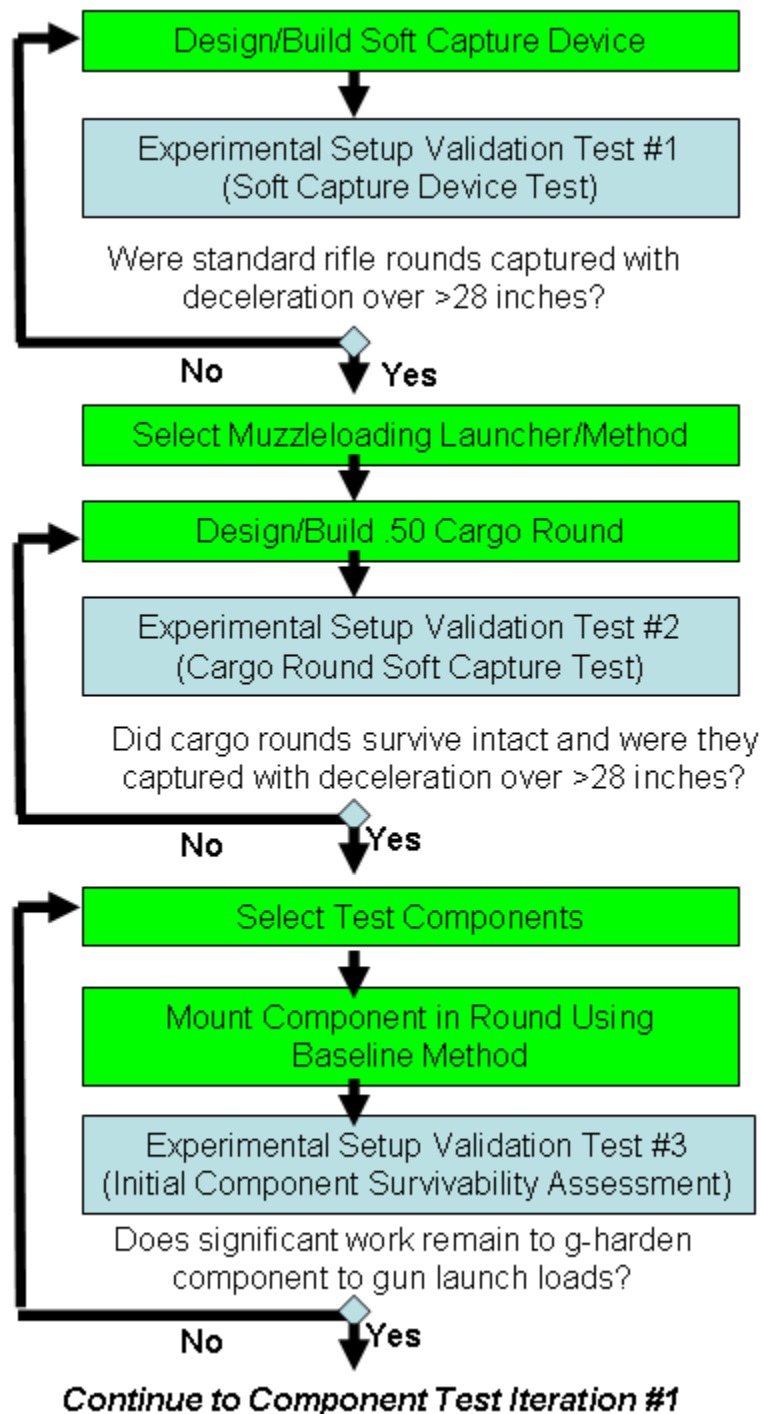
Figure 6: Experimental setup verification steps required before proceeding to component testing

3.3 Test Apparatus Detailed Descriptions

The following sections describe in detail the design of the primary apparatus used for testing.

3.3.1 Soft Capture Device

It is desirable to decelerate the projectile as slowly as possible when recovering it in order to differentiate between failure of the component upon launch versus upon impact with the target. There is no requirement for components to survive impact with the target. Several options for readily obtainable materials in which to decelerate the projectile were considered including water, ballistics gels, cardboard, sheetrock, and plywood among many others. Water is a relatively homogeneous material and therefore gives very repeatable results and does not degrade with multiple shots, however it takes a very long column of water to stop all but the lowest energy projectiles. Ballistics gels can work in shorter distances however they would likely need to be replaced after only a couple of shots. Prior experience by the author suggests that sheetrock and plywood would decelerate all but very high energy projectiles too quickly. This leaves cardboard as the remaining candidate. Cardboard is readily available and somewhere between water and sheetrock in the amount of resistance it provides to a decelerating projectile.

A 4.5 foot long box was built to hold cardboard sheets that were packed face to face the length of the box. The cross section of the box, shown in Figure 7, was 2 feet tall by 2 feet wide. The objective is to decelerate a projectile launched into the end of the box over a distance greater than the 26" barrel length of the rifle from which the projectile

would be launched. This ensures that the deceleration will be significantly less than the peak acceleration experienced in the barrel.

Figure 7: Soft capture device with top removed showing cardboard panels

Figure 8: Soft capture device prior to test

3.3.2 Cargo Rounds

A cargo round projectile is simply a bullet with a sealable interior volume in which test components can be mounted for high-g testing. Cargo rounds for this project were constructed out of both brass (C36000) and aluminum (6061-T6).   Both brass and aluminum are easily machinable but have much different densities, 8.50 g/cm^3 and 2.70 g/cm^3 respectively. This allows projectiles of the same size, but much different masses to be constructed. This is desirable to tailor the kinetic energy and momentum of rounds to ensure that they do not decelerate in the soft capture device too quickly or decelerate too slowly penetrating through the entire box and impacting the backstop.

Because aluminum can be damaging to the rifling inside of barrels a sabot design was chosen, see Figure 11. A sabot is essentially a jacket that goes around the rear of the projectile. The sabot is the diameter of the rifle bore while the projectile seated in the sabot is slightly sub-caliber and does not itself engage the rifling.

A .50 design for the projectile was chosen because it would allow it to be mounted in a .54 sabot, which is a standard caliber for muzzleloading rifles. Furthermore, .50 roundvstock in both brass and aluminum is readily available. The metric of success for the rounds is that they can be drilled out to have sufficient volume for the components of interest, while having the right mass to be captured within the soft capture device in the desired distance, all while maintaining structural integrity. It is also desirable that the rounds remain stable while traveling the short distance to the soft capture device and then for as long as possible while decelerating in the soft capture device.

Figure 9 and Figure 10 show the cargo rounds that were built. Cargo round construction was done iteratively based on lessons learned from experimental results. A total of 23 cargo rounds were constructed of six different types. Design variables between types of cargo rounds include the material, internal cavity depth, length and nose taper. Section 4.2 describes the design of the various rounds in more detail. To build the projectiles round stock was cut to the desired length, and a lathe used to cut the tapered nose, if desired, and to drill a hole from the rear of the projectile. The first several millimeters, enough for 3 threads, of the cavity were then threaded and a set screw inserted to seal the interior volume. Finally the projectile is mounted in a snug fitting .54 sabot for launch in a .54 rifle. Figure 11 shows the assembly process for a cargo round.

Figure 9: Twenty one cargo rounds used in testing, two additional rounds lost

Figure 10: Cargo rounds types from left to right; Long Al, Long Br, Short Al, Short Br, Al b2, and Br b2

Figure 11: Assembly procedure for sabot launched cargo rounds

3.3.3 Test Component Selection

Components desirable for testing were affordable COTS components that were originally

designed for more benign environments, but that may allow adaptation to high-g

conditions. Small form factor components that were identified and that meet these criteria include magnetometers, accelerometers and very small electric motors. After consideration of the relative benefit to g-hardening work with available COTS components for each, small electric motors were selected for testing. The following paragraphs describes the selection process.

Honeywell produces a commercially available magnetometer that costs $20, placing it within the cost goals of this project. In a guided projectile a magnetometer could be used to provide an on board up reference in the case of a spin stabilized projectile. The Honeywell HMC5843, Figure 12, has a 4x4x1.3mm form factor, easily fitting within a .50 round. However, it was found that very similar versions of this magnetometer are available that are rated for g-loads in the range of gun launch loads. Determining how to package the HMC5843 to also withstand those loads would represent a potential cost savings, but not a significant increase in capability versus current technology.
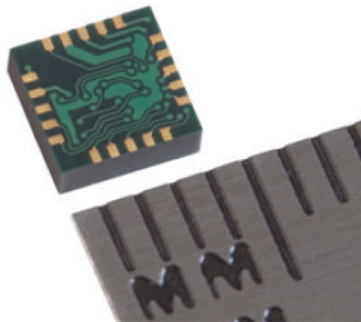
Figure 12: Honeywell HMC5843 magnetometer

Another interesting potential candidate for g-hardening is the ADXL78 accelerometer made by Analog Devices. This extremely small single axis accelerometer is made for the automotive industry to detect when an airbag should be deployed. They are mass produced and in quantity can be bought for as little as $5.66 a piece. In manufacturer specification sheets they are rated to 4,000 g's. Extending their use to 30,000 g's would

be of much interest. In guided projectiles accelerometers could be used to provide information for any internal guidance loops. Two ADXL78's were obtained for testing. However, a literature search subsequently revealed that Davis [7] had already conducted High-G experiments with the ADXL78 in support of the Army Excalibur program.

Figure 13: Analog Devices ADXL78 accelerometer

The third type of component considered for g-hardening are small electric DC motors. Electric motors could be used in a guided projectile to power many different types of actuation mechanisms in a guided projectile. Cheap COTS motors of the appropriate form factor are available. These motors are manufactured for use in RC hobby helicopters and for vibration motors in cell phones and pagers. Several different kinds of these motors were obtained for testing, see Figure 14 and Figure 15. Section 4.6 describes their electrical and physical characteristics. These motors are extremely affordable, costing as little as $0.62 when bought in single quantities. None of these motors, to the author's knowledge, have been g-hardened in any way. Furthermore, electric motors do not appear to have been used in projectiles, based on public literature, except for in the case of the WASP program which was at relatively low g's. Because of

this and their great potential benefit as cheap actuation mechanisms, electric motors were

chosen as the primary focus of the project.
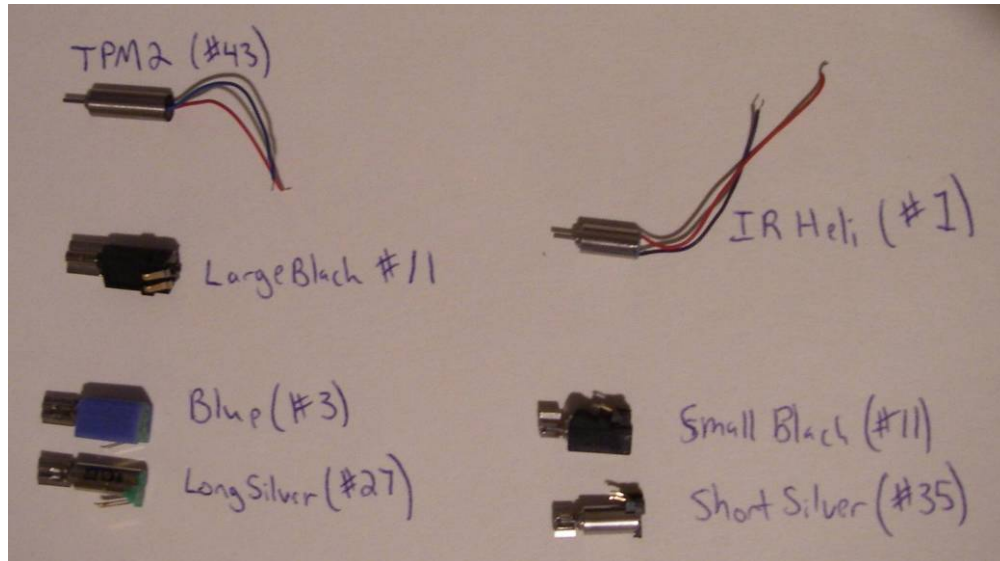
Figure 14: Five unique motor types used in testing, when casing removed #3 and #27 are identical as are #11 and #35

Figure 15: Braced type motor that was acquired but not tested

Figure 16: RC helicopter tail motor shown next to short aluminum cargo round

3.3.4 Launcher

Options for a launching device to accelerate the cargo rounds include gas guns, modern

rifles, and muzzleloaders. A gas gun uses compressed gases to accelerate a projectile

inside of a barrel. Using a gas gun the pressure of the gas and length of the impulse can be tailored to adjust the desired acceleration profile and final velocity. However, constructing a gas gun for this project or obtaining use of one such as at the facilities of the Arnold Engineering Development Center [2] [19] would be prohibitively expensive. Both modern rifles and muzzleloaders are viable options. The main difference between the two is that for a modern rifle the cargo rounds would need to be loaded into a cartridge along with the propellant and primer. This as opposed to a muzzleloader which only requires that the cargo round be loaded from the muzzle of the barrel along with the propellant. The primary advantages of a muzzleloader are that it negates the need to assemble cartridges, allows for tailoring of the powder load at the test site, and the availability of many large bore muzzleloaders available in .50, .54 and .58. The only significant drawback of using a muzzleloader is that the achievable muzzle velocities are lower compared to modern rifles. Muzzleloaders are capable of launching typical projectiles at up to 1900 ft/s, while a .50 BMG round launched from a modern rifle can obtain muzzle velocities in the range of 2800 ft/s.

Because of these advantages, it was decided to use a muzzleloader for all testing in this project. The rifle used is a .54 Connecticut Valley Arms (CVA) Eclipse Hunter model. The twist rate of the rifling is 1 turn in 32 inches and the barrel is 26 inches long. The CVA manual [3] states that FFG powder loads of up to 120 grains are safe in this rifle. Initial estimates showed that peak accelerations of up to 30,000 g's could be obtained using this rifle with a max powder load. This as compared to the approximately 65,000 g's seen by a .50 BMG round. 30,000 g's would be a representative of the launch environment seen in larger caliber artillery applications. If accelerations for testing are

desired that exceed the limits of the acceleration in the muzzleloader barrel, it is possible to use a harder material than cardboard in the capture device and use the deceleration of the cargo round as the primary shock event. In this case sheetrock would be an excellent choice as is cheap, easy to work with, and is very dense.

All tests used Hodgdons 50/50 Pyrodex Pellets as the propellant. Pyrodex is a modern alternative to blackpowder that offers higher velocities and safer handling. Each pellet is 50 grains.

For all testing, a stand was used, see Figure 17, to firmly hold the rifle in place when fired. This allows the rifle to be fired either by use of a rope or by hand keeping the head of the test operator away from the chamber. This mitigates the risk of injury in the extremely unlikely event of a malfunction with the rifle due to the custom made cargo rounds. Any malfunction is extremely unlikely since the projectile is loaded from the muzzle, as opposed to from the chamber as in a modern rifle, and therefore by definition is the proper shape to safely exit the barrel. The safety precaution of using the rifle stand was almost certainly unnecessary, but was relatively easy to implement.

Figure 17: .54 muzzleloader and rifle stand used for launching cargo rounds, soft capture device and chronograph in background

3.3.5 Ballistic Chronograph

Muzzle velocity was measured using an F-1 Ballistic Chronograph made by Shooting
Chrony Inc., see Figure 18. Ballistic chronographs are a very popular and relatively
affordable way of measuring the velocity of projectiles. This chronograph consists of
two photo sensors which sense the passing of the projectile overhead. To operate
properly the projectile must pass closely overhead of the sensors, a wire frame is
provided to outline the desired area of passing. Also, ambient light conditions must be
sufficient. The manufacturer's claimed accuracy is 99.5%.

To obtain accurate measurements, the chronograph must be placed sufficiently
downrange as to be outside the muzzle blast of the launcher. For component test
iterations #1 and #2 the chronograph was placed 10 feet downrange, and for iteration #2
14 feet downrange. In both cases it was between 4 to 5 feet from the soft capture device.
The deceleration of the projectile over this distance is negligible and the measurement by
the chronograph is therefore referred to as the muzzle velocity, despite the fact that it was
measured slightly downrange of the muzzle.

Measurement of the muzzle velocity is key to determining a reasonable estimate of the
peak g-loads experienced both in the barrel and while decelerating in the soft capture
device. For the acceleration loads experienced in the barrel the muzzle velocity can be
used, along with the barrel length, to come up with an estimated average acceleration.
This average acceleration can then be used along with available acceleration curves for
similar projectile and powder combinations to come up with an estimate of the peak g-
loads inside the barrel. The projectile also experiences non-axial balloting loads while
traveling down the barrel and setforward loads upon exit from the barrel, both of which

will be experienced but not measured or calculated. The deceleration load can be

estimated by using the muzzle velocity and material properties of the medium into which

it is launched, in this case either cardboard or sheetrock.

Figure 18: Ballistics chronograph for measuring muzzle velocity setup in front of soft capture device

3.3.6 Component Physical and Electrical Characterization Setup

Some basic tools were obtained to characterize the electric motors both before and after

launch. Shown in Figure 19, these included a lab power supply, digital calipers, small

scale and magnifying class. Specific information for the measuring devices is as follows:

- TekPower HY1803D Power Supply: 0 to 28V adjustable scale, adjustable current

- American Weigh Scales AMW-100 Digital Pocket Scale and 100 g calibration. weight: 100g capacity, 0.01g resolution.

- Generic Brand Electronic Digital Caliper: Measuring range 0-150mm, resolution 0.01mm, accuracy +- 0.02 mm (<100mm).

Figure 19: Power supply, calipers, magnifying class, and scale used for characterizing motors pre and post shock

3.4 Component Mounting for Survivability

Three basic types of mounting for gun launch load survivability were experimented with during this project. Component mounting orientation and component modifications were also varied and are discussed in Chapter 4. The three types which will be described in detail are partial encapsulation within a hard rubber well nut (Method A), encapsulation in wax (Method B), and compression mounting between washers and the cargo round set screw (Method C). Looking back the four high-g survivability techniques discussed in Chapter 2 and outlined by Berman [1] are encapsulation, underfill, load path management and component selection.   Of the mounting methods used, A and B would fall under the category encapsulation, while C would be an attempt at load path management. Several variations on these mounting methods were tried.

3.4.1 Mounting Method A: Rubber Well Nut

Method A for mounting electric motors into the cargo rounds was to seat the motor inside of a rubber well nut. Rubber well nuts were obtained of the same outer diameter as the

inner diameter of the cargo round interior cavity. The inner diameter of the well nuts are slightly smaller than most of the motors but can expand slightly creating a tight fitting seal around the motor, see Figure 20. The flange of the well nut is trimmed away and the motor inserted from the rear end, Figure 21. This has the effect of essentially encapsulating the circumference of the motor body in rubber. The axle end of the motor body is fitted snugly against the front metal end of the well nut, Figure 22, with the axle itself protruding into the hole in the nut end. The axle however is trimmed in order to not protrude outside of the well nut and impact the projectile body. The well nut is then trimmed to the length of the motor so that when the set screw is tightened it compresses the well nut and bullet assembly.

Figure 20: Rubber well nut prior to trimming and insertion into cargo round

Figure 21:   Rubber well nut mounted motor and cargo round assembly

Figure 22: Motor mounted in rubber well nut showing motor housing resting on well nut metal end with axle pointing outwards

3.4.2 Mounting Method B: Wax Encapsulant

The second method of mounting components was to encapsulate them in wax inside the cargo round. The simple setup for accomplishing this is shown in Figure 23.   Once a sufficient pool of melted wax was formed, a modified syringe was used to pull out the wax and insert it into the cavity of the projectile. It was then cooled at room temperature for between 30-60 seconds to allow the wax to partially harden before the motor was inserted into the wax to the desired depth. After the motor is inserted and the wax hardened, the end of the wax was filed down to allow the set screw to thread into the back of the cargo round. Figure 24 shows the end result.

Figure 23: Setup for wax encapsulant mounting of motors in cargo rounds

Figure 24: Rear end view of cargo round containing wax encapuslated motor

3.4.3 Mounting Method C: Compression Mount

The third type of mount was to put the axle end of the motor to be tested into a stack of washers in the fore end of the projectile. The washers were of such a diameter that the body of the motor would rest on the washer while the axle would stick out into the hole in the center of the washers. The rear end of the motor would then be fit against the set screw, see assembly view in Figure 25. The set screw was then tightened as much as possible in order to get the maximum compression possible with tightening by hand while the projectile was mounted in a vice.

Figure 25: Compression mounted (non-encapsulated) motor prior to assembly

CHAPTER 4

4 Results and Analysis

4.1 Tests

A total of 40 test launches were performed over the course of three and a half months, see timeline in Figure 26. The first three tests were necessary to incrementally evaluate the test equipment as it was being developed. These tests are referred to as Experimental Validation Tests number one through three, or V #1-3. The next three tests were full tests with the experimental setup and instrumentation developed in the prior three. These latter tests are referred to as Component Tests number one through three, or C #1-3. Table 1 shows the matrix of launches for all six tests including the projectile that was used, what component if any was mounted inside the cargo round, and any modifications to the component and the mounting method. Table 2 shows the launch measurements for all six tests, including powder load, muzzle velocity, capture result, penetration depth and medium, and whether or not a yaw card was saved from the test.

The two most important traits for a test site are a safe direction and backstop to launch towards, and an area in which the noise will not cause complaint. Tests V #1 and V #2 were conducted on remote areas in National Forest land and on a secluded beach using the ocean as a backstop. All subsequent tests were conducted on private land in Berkeley, WV where a wall of railroad ties and a large hill behind them could be used as a backstop to ensure safety should any projectiles fail to be captured in the box.
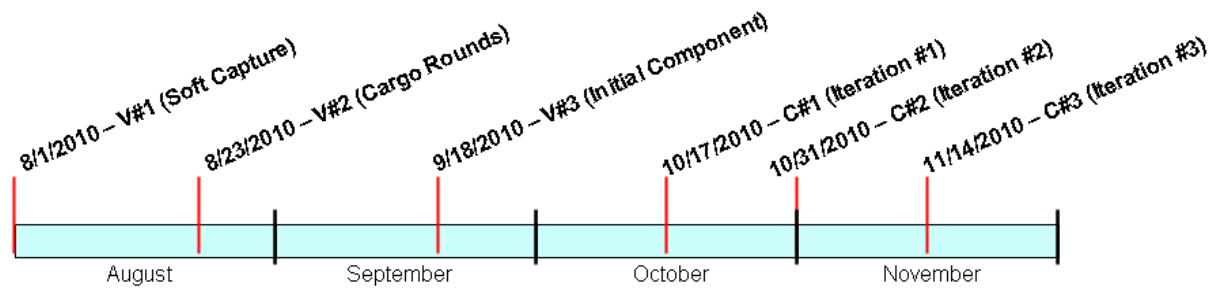
Figure 26: Timeline of experiments, August-November 2010

Table 1: Launch matrix for all tests

Test	#	Projectile	Component	Modifications	Mounting Method
V #1	1	7.62x54R	None	NA	NA
V #1	2	9mm Makarov	None	NA	NA
V #2	3	Al Short #1	None	NA	NA
V #2	4	Br Short #1	None	NA	NA
V #3	5	Al Short #2	#2 - ShIR	None	Method A: Axle Forward
V #3	6	Br Short #2	Ant	NA	Loose in cavity
V #3	7	Al Long #1	Corn Kernel	NA	Loose in cavity
C #1	8	Al Long #1	#29 - LoSi	None	Method B: Axle Forward
C #1	9	Al Long #2	#43 - LolR	None	Method B: Axle Forward
C #1	10	Al Short #1	#20 - ShSi	Weight, rubber case removed	Method B: Axle Forward
C #1	11	Al Long #3	#11 - LaBl	Weight removed	Method B: Axle Forward
C #1	12	Br Long #1	#30 - LoSi	None	Method B: Axle Rearward
C #1	13	Br Long #2	#46 - LolR	None	Method B: Axle Rearward
C #1	14	Al Short #2	#22 - ShSi	Weight, rubber case removed	Method B: Axle Rearward
C #1	15	Br Long #3	#14 - LaBl	Weight removed	Method B: Axle Rearward
C #2	16	Al Short #1	#20 - ShSi	Weight, rubber case removed	Method B: Axle Forward
C #2	17	Al Short #2	#40 - ShSi	Weight removed	Method A: Axle Forward, rear wax
C #2	18	Al Short #3	#32 - LoSi	Weight removed	Method B: Axle Forward
C #2	19	Al b2 #1	#24 - ShSi	Weight, rubber case removed	Method B: Axle Forward
C #2	20	Al b2 #2	#41 - ShSi	Weight removed	Method B: Axle Rearward
C #2	21	Al b2 #3	#23 - ShSi	Weight, rubber case removed / Rear plastic, leads, axle cut	Method B: Axle Forward
C #2	22	Al b2 #4	#25 - ShSi	Weight removed	Method B: Axle Forward
C #2	23	Al b2 #5	#9 - LoSi	Weight, forward axle removed	Method B: Axle Forward
C #2	24	Br Short #2	#10 - LoSi	Weight, forward axle removed	Method B: Axle Forward
C #2	25	Al Long #1	#42 - ShSi	Weight removed	Method B: Axle Forward
C #2	26	Br Short #3	Potato Bug	NA	Packed in dirt
C #2	27	Al b2 #6	#26 - ShSi	Weight, rubber case removed	Method C: Axle forward, 7 washers
C #2	28	Br Short #3	None	NA	NA
C #3	29	Al Short #1	#51 - ShSi	Weight, rubber case removed / JB weld rear encasement	Method B: Axle Forward
C #3	30	Al b2 #1	#76 - LoSi	Weight, rubber case, forward axle removed / JB weld rear encasement	Method B: Axle Forward
C #3	31	Al b2 #2	#87 - LoSi	Weight, forward axle removed	Method B: Axle Rearward
C #3	32	Al Short #2	#53 - ShSi	Weight, rubber case removed	Method A: Axle Forward
C #3	33	Al b2 #3	#85 - LoSi	Weight removed / Axle cut down	Method A: Axle Forward
C #3	34	Al b2 #4	#54 - ShSi	Weight, rubber case removed	Method A: Axle Rearward
C #3	35	Br b2 #1	#55 - ShSi	Weight, rubber case removed / Axle cut	Method C: Axle forward, 8 washers
C #3	36	Br b2 #2	#1 - ShIR	Leads, axle cut down	Method A: Axle Forward
C #3	37	Br b2 #3	#56 - ShSi	Weight, rubber case removed / Axle cut	Method A: Axle Forward
C #3	38	Br b2 #4	#88 - LoSi	Weight removed / Axle cut	Method A: Axle Forward
C #3	39	Al b2 #5	#57 - ShSi	Weight, rubber case removed / Axle cut	Method A: Axle Forward
C #3	40	Al Short #3	#80 - LoSi	Weight, rubber case, forward axle removed / Rear plastic, leads cut	Method A: Axle Forward

Table 2: Launch measurements for all tests

Test	#	Powder	MV	Capture Result	Yaw Card	Penetration
		Pellets	*ft/s*			
V #1	1	NA	Not Measured	Recovered in trap	No	51" Cardboard
V #1	2	NA	Not Measured	Recovered in trap	No	34" Cardboard
V #2	3	2	Not Measured	Recovered in trap	No	30" Cardboard
V #2	4	2	Not Measured	Exited trap bottom, not recovered	No	NA
V #3	5	2	Not Measured	Recovered in trap	No	29" Cardboard
V #3	6	2	Not Measured	Penetrated trap, hit backstop, recovered	No	NA
V #3	7	2	Not Measured	Recovered in trap	No	32" Cardboard
C #1	8	2	Error	Recovered in trap	No	13.5" Cardboard
C #1	9	2	1151	Recovered in trap	No	11" Cardboard
C #1	10	2	1920	Recovered in trap	No	22" Cardboard
C #1	11	2	993	Recovered in trap	No	21" Cardboard
C #1	12	2	127	Recovered in trap	No	5/8" Sheetrock x 9
C #1	13	2	129	Recovered in trap	No	5/8" Sheetrock x 11
C #1	14	2	2133	Recovered in trap	No	28.5" Cardboard
C #1	15	2	Error	Recovered in trap	No	5/8" Sheetrock x 11
C #2	16	2	239.8*	Recovered in trap	No	23" Cardboard
C #2	17	2	Error	Recovered in trap	No	24"Cardboard
C #2	18	2	Error	Recovered in trap	No	29" Cardboard
C #2	19	2	2212	Recovered in trap	No	28" Cardboard
C #2	20	2	3554*	Recovered in trap	No	20" Cardboard
C #2	21	2	2315	Recovered in trap	No	26" Cardboard
C #2	22	2	Error	Recovered in trap	No	5/8" Sheetrock x 7
C #2	23	2	Error	Recovered in trap	No	41" Cardboard
C #2	24	2	Error	Recovered in trap	No	5/8" Sheetrock x 13 / 30" Cardboard
C #2	25	2	Error	Recovered in trap	No	23" Cardboard
C #2	26	2	Error	Recovered in trap	No	5/8" Sheetrock x 13 / 39" Cardboard
C #2	27	2	Error	Exited top of trap, not recovered	No	NA
C #2	28	2	1539	Recovered in trap	No	5/8" Sheetrock x 13 / 21" Cardboard
C #3	29	2	2156	Recovered in trap	Yes	23" Cardboard
C #3	30	2	2584	Recovered in trap	Yes	30.5" Carboard
C #3	31	2	1629	Recovered in trap	Yes	22" Carboard
C #3	32	2	1955	Recovered in trap	Yes	23.5" Carboard
C #3	33	2	1867	Recovered in trap	Yes	22.5" Cardboard
C #3	34	2	1840	Recovered in trap	Yes	21.5" Cardboard
C #3	35	2	1676	Recovered in trap	Yes	37.5" Cardboard
C #3	36	2	1650	Recovered in trap	Yes	44" Cardboard / 5/8" Sheetrock x 1/2
C #3	37	1	870.4	Recovered in trap	Yes	23" Cardboard
C #3	38	1	1091	Recovered in trap	Yes	39" Cardboard
C #3	39	2	1771	Recovered in trap	Yes	5/8" Sheetrock x 7
C #3	40	2	1946	Recovered in trap	Yes	21.5" Cardboard

4.1.1 Experimental Setup Validation Tests #1 through #3

The object of the first experiment (V #1) conducted was to determine if the constructed

soft capture device was suitable for stopping projectiles of approximately the energy and

momentum of the cargo rounds that would eventually be used. To this end launches 1

and 2 launched two standard bullets into the soft capture device. These were meant to

bound the approximate lower and upper limits of what was expected for penetration by

the cargo rounds. For a low energy projectile, a 9mm Makarov round from a CZ-82 pistol was used, which penetrated 34" of cardboard. For a high energy round, a 7.62x54R round from a M44 Mosin Nagant rifle was launched, which penetrated 51" of cardboard before stopping just short of the end of the soft capture device. The desired distance for deceleration was longer than the 28" inch barrel of the muzzleloader that would be used for cargo round tests, but shorter of course than the length of the box. This would ensure that the average deceleration experienced was less than the average acceleration in the barrel of the launcher. Since both the low and high energy rounds were in the desired range for deceleration, it was decided to continue with the soft capture device as is and begin construction of cargo rounds.

The second experimental setup validation test (V #2) aimed to identify a cargo round from those produced that could be captured in the soft capture device within the desired range of penetration. Four different cargo rounds of varying masses were made for this test. The first launch of this test, launch 3, used a Short Al type round which was the lightest of the group. It penetrated 31" of cardboard which was within the desired range of 28" to 54". Launch 4 used the heavier short brass round. Unfortunately this round exited the bullet trap with considerable remaining velocity, and was not recovered. It was decided to proceed with the short aluminum cargo rounds as the baseline, since the brass cargo rounds had too much energy and the longer aluminum round was likely to have stability issues due to it's extreme length and relatively low mass.

The object of the third experiment (V #3) was to make an initial assessment of the survivability of the small motors that were identified as components of interest for high-G survivability testing. Launch 5 packaged motor #2 axle forward using Mounting

Method A, a rubber well nut. Motor #2 was not operable after launch and recovery in the soft capture device. The results of this launch and others will be discussed in detail in Section 4.6, however upon comparison to an unfired motor of the same type it was found that the shaft had shifted rearwards into the motor casing, and that when it was pulled back out the motor could partially operate. This result showed that the motor remained structurally intact enough that its basic components did not break, however it also showed that modification of the motor or mounting method, or both, was still necessary to develop a survivable package. Based on this result it was decided to proceed with procurement of additional motors of this and other types and begin systematic tests varying a number of parameters.

4.1.2 Component Test Iteration #1

The first component test iteration (C #1) launched eight cargo rounds with motors mounted inside. All eight rounds, launches 8 through 15, encapsulated the motors in wax using mounting method B. Two launches were conducted for each of four motors, one with the motor axle forward and one rearward. One motor of the eight operated after recovery, details are discussed in Section 4.6. This was also the first test that used a ballistics chronograph to measure muzzle velocity. All subsequent tests used this device.

4.1.3 Component Test Iteration #2

The second component test (C #2) launched thirteen cargo rounds, eleven of which contained motors. The primary aim of this test was to repeat the success of C #1 and if repeatable see if it can be extended to even higher g's. In the previous test it had been observed that the longer cargo rounds were tumbling prior to entry into the soft capture

device. This was evident by the oblong hole in the first sheet of cardboard. This is undesirable because high non-axial loads would be imparted on the projectile upon deceleration. Because of this a new batch of short aluminum rounds were made, type Al b2. Cargo rounds are recovered intact and can be re-used in multiple tests. The new rounds necessitated repeat tests in both the prior short aluminum rounds and Al b2 rounds. Eight launches with different motor modifications, deceleration materials, and orientation were conducted with the same Short Silver type motor as survived in test C #1. The other three launches in this test were with Long Silver type motors that had failed to survive in C #1. One launch was conducted with a new non-encapsulation method, Mounting Method C, and one other launch using Mounting Method A, but with wax to make a tighter seal around the rear of the motor. None of the motors operated after recovery, even one that was launched in the same manner as that which survived in test C #1. To determine the cause several of the motors from tests C #1 and C#2 were disassembled and it was found that wax had entered the bullet cavity, Section 4.6 discusses this issue in detail.

4.1.4 Component Test Iteration #3

Because of the failure of the wax encapsulation method in tests C #1 and C #2 to produce repeatable results, component test iteration #3 modified several motors to encase the rear portion to prevent wax flow into the casing. C #3 also opened up the trade space and re-looked at Mounting Methods A and C. A total of 12 launches were conducted for this test. Versions of all three mounting methods were investigated. The focus was on the Short Silver type motor that had survived once before in test C #1, however two other types of motors were also investigated. Two launches were also conducted with one half

of the powder load to reduce the g-loads. One launch was also done using a light cargo round and sheetrock as the deceleration material to expose it to very high deceleration loads. Four launches of this test also used a new cargo round, designated as Br b2, which was designed to be stable, while still light enough to not penetrate through the entire soft capture device. Two of the 12 launches resulted in operating motors post launch. Both of the surviving motors used Mounting Method A, one axle forward and one axle rearward, this is discussed in detail in Section 4.6.

4.2 Projectile Characterization

A total of 23 cargo rounds were made of five different types. Each one is ½ inch in diameter and made from either brass (C36000) or aluminum (6061-T6) round stock. Cargo rounds can be used many times over as they are fully intact after recovery in the soft capture device. In order to assess the energy and momentum of each round in flight and evaluate the stability, measurements were made of the mass and length of each round, shown in Table 6. Rounds were weighed empty without a set screw. Five set screws were used in total, two of which were lost and three of which were weighed at 1.63, 1.69 and 1.83 grams. Since recording of which set screw was used for each launch did not occur, an average value of 1.72 grams was used for calculations. In two cases cargo rounds were lost due to exiting the soft capture device prior to being measured; consequently no measurement data is available for those rounds. In Table 6 the asterisk next to rounds Short Al b2 #3, #4 and #5 denote that these rounds' mass changed just prior to test 3 when the depth of the cavity was increases to accommodate longer motors. The new masses are 7.26, 7.68, and 7.17 grams respectively.

Table 3: Length and mass of empty cargo rounds

Type	#	Empty Mass	Length
		g	mm
Short Al	1	6.52	28.95
Short Al	2	6.27	28.87
Short Al	3	6.67	29
Long Al	1	9.15	40.39
Long Al	2	9.2	40.6
Long Al	3	9.41	41.04
Short Br	1	NA	NA
Short Br	2	19.81	28.2
Short Br	3	21.59	29.81
Long Br	1	30.1	41.11
Long Br	2	30.22	41.32
Long Br	3	29.82	41.09
Short Al b2	1	6.78	30.35
Short Al b2	2	7.83	30.87
Short Al b2	3	7.99*	30.3
Short Al b2	4	8.16*	30.72
Short Al b2	5	7.63*	31.02
Short Al b2	6	NA	NA
Short Br b2	1	14.18	21.49
Short Br b2	2	14.1	20.38
Short Br b2	3	14.75	22.33
Short Br b2	4	15.4	22.3
Short Br b2	5	15.43	22.53

The deceleration distances for each round in either cardboard, sheetrock, or a combination of both, is shown in Table 4. For most rounds cardboard was sufficient to decelerate the projectiles with distances ranging from 11" to 42". For the Short Br and Long Br rounds however, it was necessary to use sheetrock in order to stop the projectile within the distance of the soft capture device. In order to enable deceleration within the soft capture device of Short Br rounds, launches 24, 26 and 28 were launched through 13 sheets of 5/8 inch thick sheetrock to slow their velocity. They were then decelerated to a stop through several feet of cardboard. For launch 39, a light aluminum round was decelerated in sheetrock in order to subject to extreme deceleration forces. This round decelerated from 1771 ft/s to zero in just 4.4". The result was much greater structural damage than more gently decelerated rounds; this is discussed in Section 4.6.

Table 4: Deceleration distance, launch mass, and projectile energy and momentum

Launch	Projectile	Penetration			Launch Mass***	Energy	Momentum
		Cardboard	Sheetrock				
		inches	inches		g	N*m	kg*m/s
1	7.62x54R	51	NA		14.57	NA	NA
2	9mm Makarov	34	NA		9.47	NA	NA
3	Al Short #1	30	NA		9.79	NA	NA
4	Br Short #1	NA	NA		NA	NA	NA
5	Al Short #2	29	NA		9.54	NA	NA
6	Br Short #2	NA	NA		23.08	NA	NA
7	Al Long #1	32	NA		12.42	NA	NA
8	Al Long #1	13.5	NA		12.42	NA	NA
9	Al Long #2	11	NA		12.47	7.68E+02	4.4
10	Al Short #1	22	NA		9.79	1.68E+03	5.7
11	Al Long #3	21	NA		12.68	5.81E+02	3.8
12	Br Long #1	NA	5.6		33.37	2.50E+01	1.3
13	Br Long #2	NA	6.9		33.49	2.59E+01	1.3
14	Al Short #2	28.5	NA		9.54	2.02E+03	6.2
15	Br Long #3	NA	6.9		33.09	NA	NA
16	Al Short #1	23	NA		9.79	2.62E+01	0.7
17	Al Short #2	24	NA		9.54	NA	NA
18	Al Short #3	29	NA		9.94	NA	NA
19	Al b2 #1	28	NA		10.05	2.29E+03	6.8
20	Al b2 #2	20	NA		11.10	6.52E+03	12.0
21	Al b2 #3	26	NA		11.26	2.80E+03	7.9
22	Al b2 #4	NA	4.4		11.43	NA	NA
23	Al b2 #5	41	NA		10.90	NA	NA
24	Br Short #2	30	8.1	*	23.08	NA	NA
25	Al Long #1	23	NA		12.42	NA	NA
26	Br Short #3	39	8.1	*	24.86	NA	NA
27	Al b2 #6	NA	NA		NA	NA	NA
28	Br Short #3	21	8.1	*	24.86	2.74E+03	11.7
29	Al Short #1	23	NA		9.79	2.11E+03	6.4
30	Al b2 #1	30.5	NA		10.05	3.12E+03	7.9
31	Al b2 #2	22	NA		11.10	1.37E+03	5.5
32	Al Short #2	23.5	NA		9.54	1.69E+03	5.7
33	Al b2 #3	22.5	NA		11.26	1.82E+03	6.4
34	Al b2 #4	21.5	NA		11.43	1.80E+03	6.4
35	Br b2 #1	37.5	NA		17.45	2.28E+03	8.9
36	Br b2 #2	44	0.3	**	17.37	2.20E+03	8.7
37	Br b2 #3	23	NA		18.02	6.34E+02	4.8
38	Br b2 #4	39	NA		18.67	1.03E+03	6.2
39	Al b2 #5	NA	4.4		10.90	1.59E+03	5.9
40	Al Short #3	21.5	NA		9.94	1.75E+03	5.9

*Penetrated sheetrock then continued through cardboard

**Penetrated cardboard then continued through sheetrock

***Mass based on empty cargo round mass plus average set screw (1.72g) and average motor/mounting material combination (1.55g)

Also shown in Table 4 is the calculated kinetic energy and momentum for every launch in which a muzzle velocity measurement was made. Muzzle velocity is then plotted versus both in Figure 27 and Figure 28. Launches 16 and 20 were not plotted due to erroneous velocity measurements. For the launches into cardboard with Short Al, Short Al b2, and Long Al cargo rounds the data shows a strong correlation between deceleration distance and both kinetic energy and momentum. For those rounds launched into only sheetrock, some of the Long Brass and one Short Al b2 round, there are too few launches to draw many conclusions. For the Short Br b2 shots that used only ½ of the normal powder load the energy and momentum was much lower, as would be expected, but the fall off in deceleration distance was not as apparent. These and other differences can likely be explained by the non-uniformity of the cardboard, especially after several rounds had been stopped without changing the cardboard sheets. Efforts were made during testing to launch the rounds into different areas of the soft capture device to avoid one projectile traveling in the path of a previous one, however some reduced resistance may have occurred. The Long Br, Long Al and some of the Short Al and Al b2 launches were likely tumbling prior to entering the soft capture device which would create increased resistance and shorten the deceleration distance. The Short Brass b2 rounds were designed to be very stable in flight and this may explain why they tended to go further than would be expected for rounds of their energy and momentum. Launches 28 and 36 were not plotted despite having valid velocity measurements since they involved deceleration in a mixture of sheetrock and cardboard.
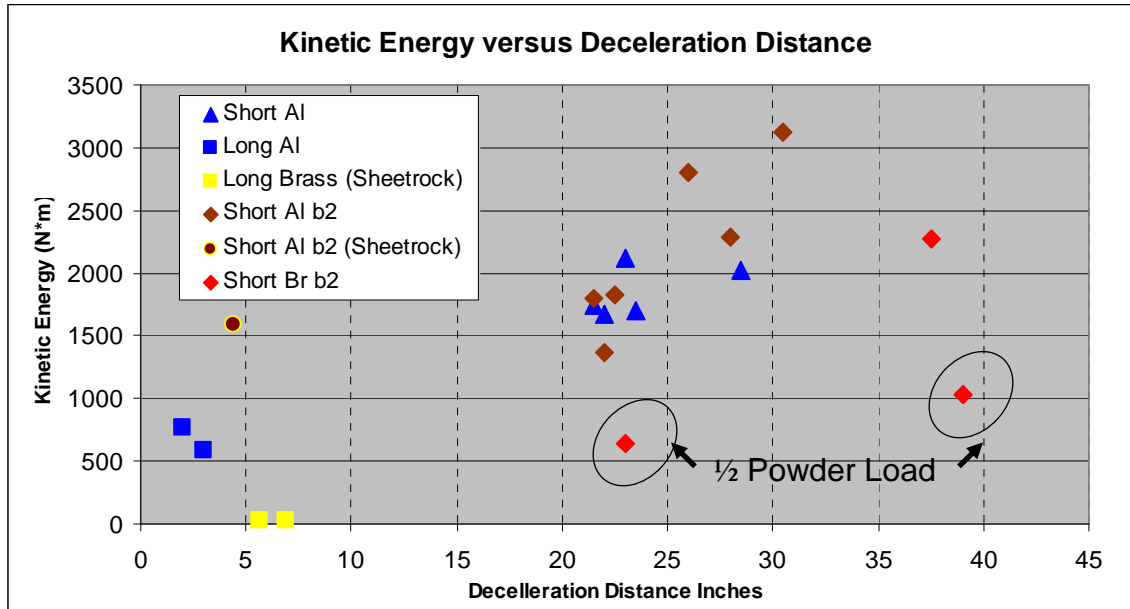
Figure 27: Kinetic energy versus deceleration distance
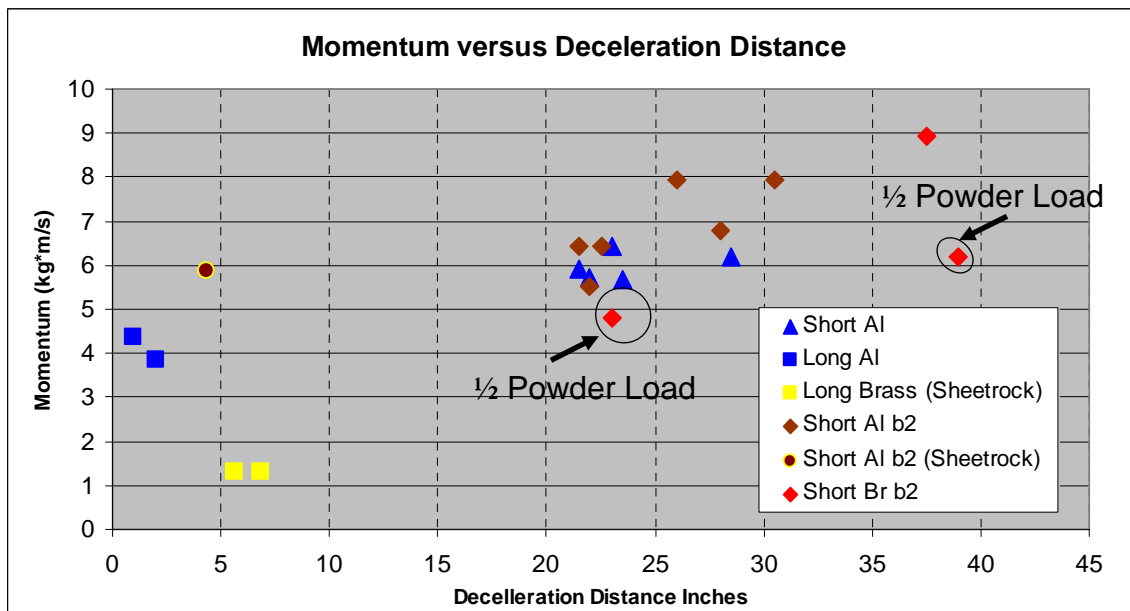
Figure 28: Momentum versus deceleration distance

4.3 Achieved G-Loading

In order to experimentally assess the ability of the tested components to survive gun

launch loads, it is necessary to know the g-loads experienced during the test launches.

The ability to measure projectile in-barrel acceleration directly was not available to this

project. In order to come up with a reasonable estimate of the peak acceleration,

measurements of muzzle velocity, along with the known barrel length were used to calculate an average in barrel acceleration. The average acceleration for the cargo rounds was then compared to the calculated average accelerations for several other gun launched projectiles. The known peak in barrel acceleration for the standard rounds was then compared to their calculated average accelerations and used to apply a correction to the calculated average accelerations for the cargo round launches.

In order to calculate an average acceleration from muzzle velocity and barrel length, a simplification must be made and a constant acceleration assumed throughout the length of the barrel. Since the typical acceleration curve, as exemplified in Figure 3, is close to symmetrical about its peak, this is a reasonable simplification for these calculations. Assuming constant acceleration, the average acceleration can be calculated as follows:

$$V_{ave} = \frac{1}{2}(V_0 + V_{muzzle}) \tag{1}$$

$$t = \frac{L_{barrel}}{V_{ave}} \tag{2}$$

$$A_{ave} = \frac{(V_{muzzle} - V_0)}{t} \tag{3}$$

Combining terms and using the fact that the initial velocity, V_0, is zero the previous equations can be simplified as follows:

$$A_{ave} = \frac{V_{muzzle}^2}{2 * L_{barrel}} \tag{4}$$

Using this equation for the average acceleration, A_{ave}, the average acceleration for three standard rounds was calculated, shown in Table 5. The M33 50-caliber round is the closest analogy to the cargo rounds used for this experiment. The barrel length and

muzzle velocities are fairly close. The main difference is that the M33 is a much heavier round than the relatively light brass, and especially the aluminum rounds made for this project. It is also propelled by modern smokeless powder, as opposed to Pyrodex. For a description of Pyrodex and other modern blackpowder substitutes refer to Rinker [18]. For purpose of estimating the shape of the acceleration curve, burn rate is the important propellant characteristic to consider. As discussed in Gonzalez [11], starting on page 41, burn rate is a function of the shape of the propellant grains. Unfortunately data on the burn rate of Pyrodex is not published, and the M33 remains the best analogy. Also looked at are the M830A1 round used on the M1 Abrams tank main gun [5] and an ultra high velocity test round used in experiments at Oakridge Labs [20]. The ratio of the peak to calculated average in barrel accelerations for the M33, M830A1 and Oakridge Labs round were 1.3, 1.7, and 5.5 respectively, see Table 5. The much larger value for the Oakridge Labs round is believed to be related to the much higher velocity of that round which was over five times that of the M33.

Table 5: Peak vs. average in barrel accelerations for several different rounds [5] [20]

	M33	M830A1	Oakridge Labs Test	Cargo Rounds
Projectile Diameter	0.50	120 mm	3.9 mm	0.50
Launcher	M107	M256	Gas Gun	CVA Eclipse
Barrel Length (inches)	29	209	39	26
Barrel Length (m)	0.74	5.30	1.00	0.66
Muzzle Velocity (ft/s)	2798	4592	14760	Variable
Muzzle Velocity (m/s)	853	1400	4500	Variable
Average Accel (g's)	50300	18800	1030000	Variable
Peak Accel. (g's)	65000	32000	5710000	Calculated
Peak/Average Accel.	1.3	1.7	5.5	Calculated

Figure 29 shows the measured muzzle velocities for all launches conducted for this project. The data is separated by cargo round type. Prior to launch number 28 the ballistics chronograph was used in less than optimum lighting conditions leading to a failure to measure muzzle velocity for several shots. Component test iterations #1 and #2 were conducted in late afternoon when the sun was relatively low. For component test #3, which started with launch 28, the launches were all done at midday with a clear sky and no failures to take measurements occurred. During the tests with poor lighting conditions, two measurements were taken that are extreme outliers. Both of these launches saw average, as compared to launches with the same cargo round type, penetration of the soft capture device. Therefore, it is believed that the measurement is in error. These erroneous measurements are marked as such in Figure 29.

Overall the muzzle velocity measurements appear consistent with one another. The variation in muzzle velocities seen within launches of the same cargo round type could easily be explained by differences in projectiles, varying friction in the barrel as fouling builds up, degree to which the projectile compressed the propellant when loaded, or other factors. For two launches where the powder load was halved, launches 37 and 38, a marked reduction in muzzle velocity is apparent.
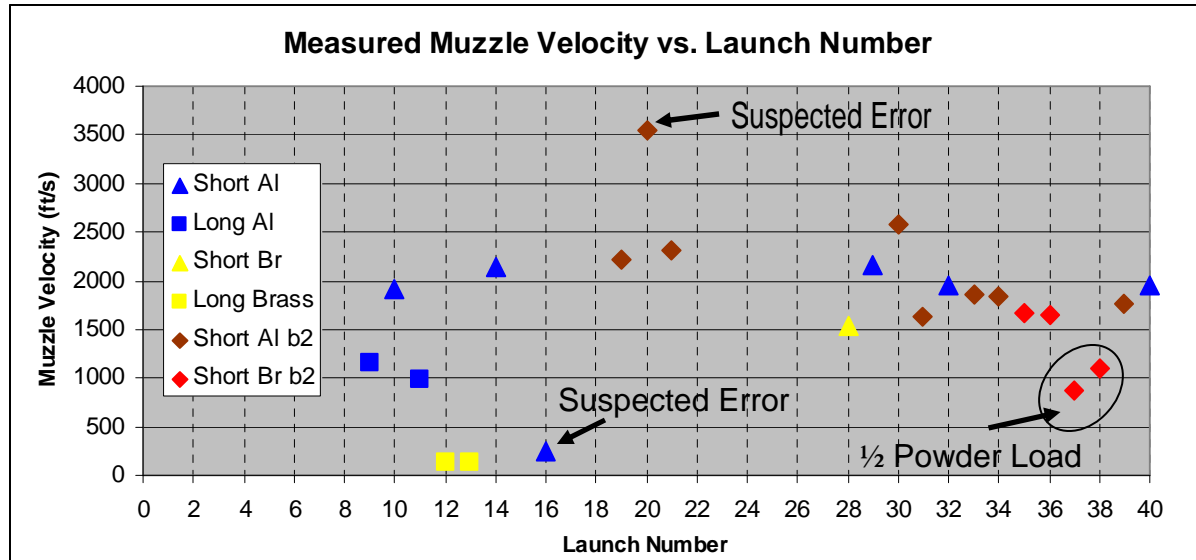
Figure 29: Chronograph measured muzzle velocities

Shown in Figure 30 are the calculated average accelerations using Equation 4 and the measured muzzle velocities shown in Figure 29. As shown in Table 5, the closest standard projectile to the cargo rounds for which a peak acceleration was available is the M33 .50 round. The M33 has a ratio of measured peak acceleration to average in-barrel acceleration, as calculated by Equation 4, of 1.3. Because of the slightly lower muzzle velocities of the cargo rounds used for this project, it is believed that that ratio would be somewhat lower, but would not be of course less than one. As such, the peak acceleration is assumed to be approximately 1.2 times the estimated average acceleration. This 20% range is shown as positive error bars in Figure 30.

Table 6 shows the numeric values plotted in Figure 29 and Figure 30. Looking at the table, it can be seen that a modest increase in muzzle velocity can lead to a proportionately larger increase in peak acceleration experienced. The estimated highest achieved in barrel acceleration was in launch 30 at just over 57,000 g's. This data will be used in section 4.6 and 4.7 when the post launch measurements of the motors are discussed.
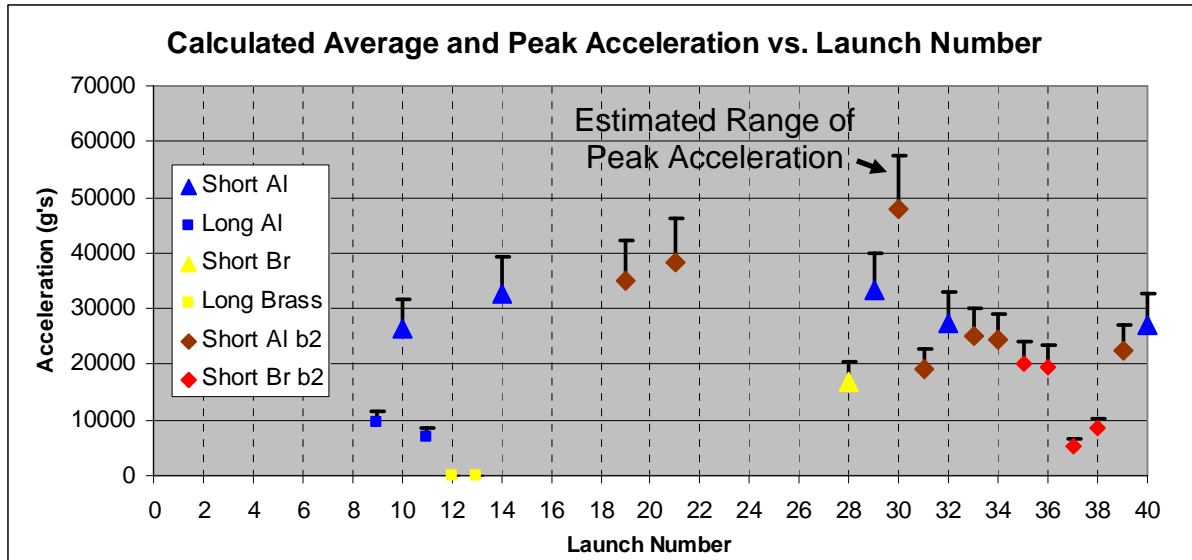
Figure 30: Calculated average and range of peak accelerations based on chronograph measurements and comparison to standard rounds

Table 6: Measured muzzle velocity and calculated average and peak accelerations using 1.2 correction factor

Launch	Projectile	Powder	Muzzle Velocity	Average Accel	Est. Peak Accel
		Pellets	ft/s	G's	G's
9	Al Long #2	2	1151	9504	11405
10	Al Short #1	2	1920	26445	31734
11	Al Long #3	2	993	7074	8488
12	Br Long #1	2	127	116	139
13	Br Long #2	2	129	119	143
14	Al Short #2	2	2133	32638	39166
19	Al b2 #1	2	2212	35101	42121
21	Al b2 #3	2	2315	38446	46135
28	Br Short #3	2	1539	16991	20389
29	Al Short #1	2	2156	33346	40015
30	Al b2 #1	2	2584	47900	57479
31	Al b2 #2	2	1629	19037	22844
32	Al Short #2	2	1955	27418	32902
33	Al b2 #3	2	1867	25005	30007
34	Al b2 #4	2	1840	24287	29145
35	Br b2 #1	2	1676	20151	24181
36	Br b2 #2	2	1650	19531	23437
37	Br b2 #3	1	870.4	5435	6522
38	Br b2 #4	1	1091	8539	10247
39	Al b2 #5	2	1771	22500	27000
40	Al Short #3	2	1946	27166	32600

4.4 Projectile Stability

In a guided projectile, and also in the cargo rounds built for this project, stability is a more challenging design driver than in standard rounds. An unstable projectile would of course have very poor accuracy. Stability is more of a challenge because of the large internal volume that is taken up by electronics and actuators in a guided projectile, as opposed to the much denser lead or steel core of standard projectiles. To increase stability, a guided projectile design can do one or more of several things: incorporate denser materials such as tungsten, shrink in length, spin faster, control stability aerodynamically, or give up margin. Similarly, the cargo rounds constructed for this project, which were made out of light materials and had large hollow interior volumes, must be designed with stability in mind but for different reasons than accuracy.

In order to limit deceleration loads that may cause damage to components that would be indistinguishable from any damage occurring during launch, it is desirable to use a cargo round that is as stable as possible in flight. Should the projectile be tumbling upon entry into the soft capture device, potentially high non-axial loads would be experienced as the projectile rotates end over end while decelerating. The more stable the projectile, the longer it will remain in a nose forward orientation while decelerating inside the soft capture device. Eventually it will begin to tumble as the velocity decreases, however at this point the rate of deceleration would have decreased significantly since initial entry.

In order to increase projectile stability, one can increase velocity, spin rate or mass, or decrease length. Since the rifling twist rate of the launcher is fixed and velocity is directly related to the launch loads experienced, the knobs available here are projectile length and mass.

The most common way of determining projectile stability is to use a simple yaw card, or set of yaw cards. A yaw card is merely a sheet of material, usually cardboard or paper, through which the projectile is shot. The shape of the hole in the yaw card can indicate whether or not at that point the projectile was flying straight, yawed at an angle, or tumbling. The first sheet of cardboard or sheetrock in the soft capture device used for this project is essentially a built in yaw card. For launches 1 through 28 occasional notes were made of the shape of the holes in the first cardboard sheet. Unfortunately this was not done in a systematic way and yaw cards results are not available for all launches. For launches 29-40 a new sheet of cardboard was used as a yaw card for each launch and photographs of each can be seen in Appendix A. The results for all observations are summarized in Table 7.

As can be seen in Table 7 the longer rounds, Long Br and Long Al, tumbled on every recorded launch. As a result, these rounds were not used in later tests. The short aluminum rounds, Short Al and Al b2 series, experienced mixed results with some rounds such as Al b2 #1, Al b2#3, and Al b2 #5 appearing stable while others such as Al Short #1, Al Short #2, and Al b2 #4 appeared consistently unstable. Because of these results a new type of round for component test #3 was made. The Br b2 series rounds were made as short as possible, between 20.4 to 22.5 mm, while still having sufficient cargo space for the smallest motors. Furthermore, this round being made of brass was significantly heavier than the aluminum rounds, in the range of 14 to 15 grams as opposed to 6 to 8. The result was a round with much greater stability that based on post launch observation of the traveled path appeared not to tumble until well through most of the soft capture

device. See Appendix A for a comparison of yaw card results for stable and unstable

rounds.

Table 7: Summary of projectile stability for launches with recorded yaw card results

Launch	Projectile	Stabilty	Data Source
1	7.62x54R	Stable	Notes
2	9mm Makarov	Stable	Notes
3	Al Short #1		NA
4	Br Short #1		NA
5	Al Short #2		NA
6	Br Short #2		NA
7	Al Long #1		NA
8	Al Long #1	Tumbling	Notes
9	Al Long #2	Tumbling	Notes
10	Al Short #1		NA
11	Al Long #3	Tumbling	Notes
12	Br Long #1	Tumbling	Notes
13	Br Long #2	Tumbling	Notes
14	Al Short #2		NA
15	Br Long #3	Tumbling	Notes
16	Al Short #1	Tumbling	Notes
17	Al Short #2	Tumbling	Notes
18	Al Short #3		NA
19	Al b2 #1	Stable	Notes
20	Al b2 #2		NA
21	Al b2 #3		NA
22	Al b2 #4	Tumbling	Notes
23	Al b2 #5	Stable	Notes
24	Br Short #2		NA
25	Al Long #1		NA
26	Br Short #3		NA
27	Al b2 #6		NA
28	Br Short #3	Stable	Yaw Card Picture
29	Al Short #1	Tumbling	Yaw Card Picture
30	Al b2 #1	Stable	Yaw Card Picture
31	Al b2 #2	Unclear	Yaw Card Picture
32	Al Short #2	Tumbling	Yaw Card Picture
33	Al b2 #3	Stable	Yaw Card Picture
34	Al b2 #4	Tumbling	Yaw Card Picture
35	Br b2 #1	Stable	Yaw Card Picture
36	Br b2 #2	Stable	Yaw Card Picture
37	Br b2 #3	Stable	Yaw Card Picture
38	Br b2 #4	Stable	Yaw Card Picture
39	Al b2 #5	Stable	Yaw Card Picture
40	Al Short #3	Tumbling	Yaw Card Picture

4.5 Pre-Launch Motor Characterization

A total of 90 small COTS DC motors were obtained for evaluation. Thirty-one of these

were launched in cargo rounds during testing, with one of them being launched twice.

The primary objective of this project is to identify low cost motors of the correct form factor and g-harden them for small caliber gun launch loads. Due to the high volume production rate of small caliber bullets, and the one time use nature of the product, affordability is a major driver. The motors for this project were acquired from public sources at retail prices in four different orders. The following shows the sources and costs of each order, including shipping, of each lot of motors.

- 9/6/10 - Amazon.com ($23.89) – Motors 1 and 2
- 9/23/10 - The Electronics Goldmine ($24.87) – Motors 3 through 42
- 9/23/10 - Solarbotics ($42.14) – Motors 43 through 50
- 11/4/10 – The Electronics Goldmine ($33.87) – Motors 51 through 90

Appendix B lists all 90 motors and the pre-modification electrical and physical properties of those that were measured. The cost of each motor is also shown. Cost is based on the total cost of the order divided by the number of motors obtained in that order. Cost per motor varied from $0.62 to $11.95. In the case of motors 1 and 2, labeled here as "IR Heli", the intended application is as tail motors for small radio controlled helicopters. Motors 43 through 50 are called "TPM2" based on the TPM2 stamp on their packaging and they appear to be longer versions of the IR Heli type motors, however their intended use is unknown. All other motors are manufactured for use as vibration motors in cell phones and pagers. These are readily identifiable by the relatively heavy off axis weight mounted on the end of the axle.

It should be noted that when cases and vibration weights were removed, several types of motors that initially appeared different turned out to be the same motor in different packaging. In Appendix B, the "Type" column denotes the type of motor when all casing

is removed. However, the "Lot / Casing" column tracks what the original packaging was for motors believed to otherwise be identical. In the case of the two orders from Electronics Goldmine a quantity of eight of the same package of five different motors was ordered on two different occasions. However, the types of motors received varied. Motors received in the second order are denoted with an "o2" in Appendix B.

4.6 Component Post Launch Results and Analysis

There were 32 launches, out of a total of 40, with motors mounted inside. The remaining launches were either tests of the soft capture device, the cargo rounds themselves, or in a couple of cases, discussed in Appendix D, investigated unrelated questions. In one launch the cargo round, with motor inside, failed to be captured, leaving 31 total recovered motors for analysis. For purpose of comparing results and drawing conclusions, seven variables for each launch are looked at:

1) Type of Motor

2) Modifications to the Motor

3) Mounting Method

4) Launch Loads

5) Deceleration Distance and Material

6) Whether or Not Projectile was Tumbling Upon Entering Soft Capture Device

7) Test Day Conditions

Table 8 shows these variables for the 31 launches with recovered motors. In cases where yaw cards were not observed, stability is estimated by looking at results for launches with the same projectile at approximately the same speed, when available. For launches in which no muzzle velocity measurement was successfully obtained the peak acceleration

is estimated in a similar manner. All table entries estimated from other launches, as opposed to measured for that launch, are denoted in blue italic text. Table 9 shows the measurements for each recovered motor, prior to and after launch, including whether or not that motor was functioning. Pre-launch electrical and physical measurements of motors can be found in Appendix C.

Table 8: Selected variables for launches resulting in recovered motors

#	Projectile	Motor	Modifications	Mounting Method	Est. Peak G	Cardboard	Sheetrock	Stabilty
					G's	inches	inches	
5	Al Short #2	#2 - ShIR	None	Method A: Axle Forward	39000	29	NA	Tumbling
8	Al Long #1	#29 - LoSi	None	Method B: Axle Forward	11000	13.5	NA	Tumbling
9	Al Long #2	#43 - LoIR	None	Method B: Axle Forward	11405	11	NA	Tumbling
10	Al Short #1	#20 - ShSi	Weight, rubber case removed	Method B: Axle Forward	31734	22	NA	Tumbling
11	Al Long #3	#11 - LaBl	Weight removed	Method B: Axle Forward	8488	21	NA	Tumbling
12	Br Long #1	#30 - LoSi	None	Method B: Axle Rearward	139	NA	5.6	Tumbling
13	Br Long #2	#46 - LoIR	None	Method B: Axle Rearward	143	NA	6.9	Tumbling
14	Al Short #2	#22 - ShSi	Weight, rubber case removed	Method B: Axle Rearward	39166	28.5	NA	Tumbling
15	Br Long #3	#14 - LaBl	Weight removed	Method B: Axle Rearward	140	NA	6.9	Tumbling
16	Al Short #1	#20 - ShSi	Weight, rubber case removed	Method B: Axle Forward	40000	23	NA	Tumbling
17	Al Short #2	#40 - ShSi	Weight removed	Method A: Axle For., rear seal	33000	24	NA	Tumbling
18	Al Short #3	#32 - LoSi	Weight removed	Method B: Axle Forward	33000	29	NA	Unclear
19	Al b2 #1	#24 - ShSi	Weight, rubber case removed	Method B: Axle Forward	42121	28	NA	Stable
20	Al b2 #2	#41 - ShSi	Weight removed	Method B: Axle Rearward	23000	20	NA	Unclear
21	Al b2 #3	#23 - ShSi	Weight, case removed / Rear plastic, leads, axle cut	Method B: Axle Forward	46135	26	NA	Stable
22	Al b2 #4	#25 - ShSi	Weight removed	Method B: Axle Forward	29000	NA	4.4	Tumbling
23	Al b2 #5	#9 - LoSi	Weight, forward axle removed	Method B: Axle Forward	27000	41	NA	Stable
24	Br Short #2	#10 - LoSi	Weight, forward axle removed	Method B: Axle Forward	20000	30	8.1*	Stable
25	Al Long #1	#42 - ShSi	Weight removed	Method B: Axle Forward	11000	23	NA	Tumbling
29	Al Short #1	#51 - ShSi	Weight, rubber case removed / JB weld encasement	Method B: Axle Forward	40015	23	NA	Tumbling
30	Al b2 #1	#76 - LoSi	Weight, case, forward axle removed / JB weld encasement	Method B: Axle Forward	57479	30.5	NA	Stable
31	Al b2 #2	#87 - LoSi	Weight, forward axle removed	Method B: Axle Rearward	22844	22	NA	Unclear
32	Al Short #2	#53 - ShSi	Weight, rubber case removed	Method A: Axle Forward	32902	23.5	NA	Tumbling
33	Al b2 #3	#85 - LoSi	Weight removed / Axle cut down	Method A: Axle Forward	30007	22.5	NA	Stable
34	Al b2 #4	#54 - ShSi	Weight, rubber case removed	Method A: Axle Rearward	29145	21.5	NA	Tumbling
35	Br b2 #1	#55 - ShSi	Weight, rubber case removed / Axle cut	Method C: Axle For., 8 washers	24181	37.5	NA	Stable
36	Br b2 #2	#1 - ShIR	Leads, axle cut down	Method A: Axle Forward	23437	44*	0.3	Stable
37	Br b2 #3	#56 - ShSi	Weight, rubber case removed / Axle cut	Method A: Axle Forward	6522	23	NA	Stable
38	Br b2 #4	#88 - LoSi	Weight removed / Axle cut	Method A: Axle Forward	10247	39	NA	Stable
39	Al b2 #5	#57 - ShSi	Weight, rubber case removed / Axle cut	Method A: Axle Forward	27000	NA	4.4	Stable
40	Al Short #3	#80 - LoSi	Weight, case, forward axle removed / Rear , leads cut	Method A: Axle Forward	32600	21.5	NA	Tumbling

* Denotes material through which projectile first decelerated (either cardboard or sheetrock)

example = Blue/Italic font indicates quantity was estimated from measurements of similar launches

Table 9: Post launch results for launches with recovered motors

Launch	Component	Operates	Visible Damage	Voltage	Current
				V	A
5	#2 - ShIR	No	Shaft pushed back into casing slightly	3.7	0.11
8	#29 - LoSi	Partial Turn	None	3.7	0.06
9	#43 - LoIR	No	None	3.7	0.03
10	#20 - ShSi	Yes	None	3.7	0.07
11	#11 - LaBl	No	None	3.7	0
12	#30 - LoSi	No	Weight and axle bent	3.7	0
13	#46 - LoIR	No	Rear of motor caved in	3.7	0
14	#22 - ShSi	No	None	3.7	0
15	#14 - LaBl	No	None	3.7	0
16	#20 - ShSi	No	None	3.7	0
17	#40 - ShSi	No	None	3.7	0
18	#32 - LoSi	No	None	3.7	0
19	#24 - ShSi	No	None	3.7	0
20	#41 - ShSi	No	None	3.7	0
21	#23 - ShSi	No	None	3.7	0
22	#25 - ShSi	No	Axle bent and jammed into case	3.7	0
23	#9 - LoSi	No	None	3.7	0
24	#10 - LoSi	No	None	3.7	0
25	#42 - ShSi	No	None	3.7	0
29	#51 - ShSi	No	None / Initially pulls 0.25 A then quickly falls to 0.00	3.7	0
30	#76 - LoSi	No	None	3.7	0.08
31	#87 - LoSi	No	Leads bent	3.7	0
32	#53 - ShSi	Yes	None / Operates, sounds high pitched	3.7	0.1
33	#85 - LoSi	No	None	3.7	0
34	#54 - ShSi	Yes	None / Operates, sounds high pitched	3.7	0.07
35	#55 - ShSi	No	Washers undamaged, rear of motor deformed inwards, front appears intact, motor loose in bullet	3.7	Max (3.04)
36	#1 - ShIR	No	Rear deformed inwards	3.7	0.13
37	#56 - ShSi	No	None	3.7	0.25
38	#88 - LoSi	No	Rear of plastic and motor deformed inwards	3.7	Max (3.04)
39	#57 - ShSi	No	Al. bullet splinters behind motor, part of plastic rear broke off, windings and axle ejected forward	3.7	Max (3.04)
40	#80 - LoSi	No	Rear deformed	3.7	Max (3.04)

For motors that sustained significant visible damage the length, width and mass of the

motors was measured post launch. This information is shown in Table 10.

Table 10: Post launch measurements for motors with significant visible damage

Launch	Length	Width	Mass
	mm	mm	g
35	10.26	6.28	0.43
36	10.26	4.35	0.45
37	12.91	5.58	0.55
39	12.45	NA	NA

4.6.1 Post Launch Operating Motors

Five launches resulted in recovered motors that operated fully or partially. The launch

parameters are shown in Table 11 and specific post launch component results in Table 9.

In the case of launch 5, the Short IR type motor did not operate after recovery until the

shaft which had been forced backwards by the shock was pulled out. In launch 8 the

recovered Long Silver type motor could make only a partial rotation, furthermore the

launch saw an estimated only 11,000 g's. However, launches 10, 32, and 34 saw Short

Silver type motors survive launch loads in the range of 29,000 to almost 33,000 g's. The

Short Silver type motors were the only motor of the five types launched that resulted in

any fully functioning post launch and recovery. The next several sections will compare

these launches with launches using similar methods that did not result in operating

motors.

Table 11: Variables for launches with partial of fully operating recovered motors

#	Projectile	Motor	Modifications	Mounting Method	Est. Peak G	Cardboard	Sheetrock	Stabilty
					G's	*inches*	*inches*	
5	Al Short #2	#2 - ShIR	None	Method A: Axle Forward	*39000*	29	NA	*Tumbling*
8	Al Long #1	#29 - LoSi	None	Method B: Axle Forward	*11000*	13.5	NA	Tumbling
10	Al Short #1	#20 - ShSi	Weight, rubber case removed	Method B: Axle Forward	31734	22	NA	*Tumbling*
32	Al Short #2	#53 - ShSi	Weight, rubber case removed	Method A: Axle Forward	32902	23.5	NA	Tumbling
34	Al b2 #4	#54 - ShSi	Weight, rubber case removed	Method A: Axle Rearward	29145	21.5	NA	Tumbling

4.6.2 Mounting Method A

Table 12 and Table 13 show the launch parameters for all launches that involved a

payload mounted using Mounting Method A and launched with a standard two Pyrodex

pellet powder load. Mounting Method A uses a carefully sized rubber well nut to encase

the motor in the cargo round as described in Section 3.4.1.

Table 12: Parameters for Mounting Method A launches with standard powder loads

#	Projectile	Motor	Modifications	Mounting Method	Est. Peak G	Cardboard	Sheetrock	Stabilty
					G's	inches	inches	
5	Al Short #2	#2 - ShIR	None	Method A: Axle Forward	39000	29	NA	Tumbling
17	Al Short #2	#40 - ShSi	Weight removed	Method A: Axle For., rear seal	33000	24	NA	Tumbling
32	Al Short #2	#53 - ShSi	Weight, rubber case removed	Method A: Axle Forward	32902	23.5	NA	Tumbling
33	Al b2 #3	#85 - LoSi	Weight removed / Axle cut down	Method A: Axle Forward	30007	22.5	NA	Stable
34	Al b2 #4	#54 - ShSi	Weight, rubber case removed	Method A: Axle Rearward	29145	21.5	NA	Tumbling
36	Br b2 #2	#1 - ShIR	Leads, axle cut down	Method A: Axle Forward	23437	44*	0.3	Stable
40	Al Short #3	#80 - LoSi	Weight, case, forward axle removed / Rear , leads cut	Method A: Axle Forward	32600	21.5	NA	Tumbling

Table 13: Results for Mounting Method A launches with standard powder loads

Launch	Component	Operates	Visible Damage	Voltage	Current
				V	A
5	#2 - ShIR	No	Shaft pushed back into casing slightly	3.7	0.11
17	#40 - ShSi	No	None	3.7	0
32	#53 - ShSi	Yes	None / Operates, sounds high pitched	3.7	0.1
33	#85 - LoSi	No	None	3.7	0
34	#54 - ShSi	Yes	None / Operates, sounds high pitched	3.7	0.07
36	#1 - ShIR	No	Rear deformed inwards	3.7	0.13
40	#80 - LoSi	No	Rear deformed	3.7	Max (3.04)

The first launch to use Mounting Method A was number 5, which launched a Short IR type motor in an axle forward configuration as shown in Figure 31. No chronograph measurement was available for this early launch, but by comparison to later launches, with the same cargo round, the estimated peak g's are 39,000. This motor did not operate after launch. With the axle seized the motor pulled 0.11A, as opposed to 0.01A nominal, and became hot very quickly. Upon comparison with an un-launched motor, it was noticed that the shaft had been forced rearward by the launch loads approximately 1/3 of its length, see Figure 32. When the shaft was pulled out with a small pair of pliers, the motor operated. However, the motor pulled more current than it had pre-launch, 0.02A compared to 0.01A, and made a distinctively higher pitch noise when operating. If tilted upwards the axle would slide back into the casing and the motor would again seize. Launch 36 also used a Short IR type motor in an axle forward configuration. However, this launch resulted in the rear of the motor deforming against the set screw and the motor pulling 0.13A and not operating post launch. This result is unexpected as the estimated launch loads for launch 36 are actually less than that for launch 5. However, in launch 5 the motor was much less damaged. The damage is unlikely to have occurred during

deceleration as it is in the rear of the motor and the projectile used for launch 36 was stable. The believed likely cause is improper mounting such as not compressing the motor tightly enough against the front of the well nut via the set screw. This could have led to movement of the motor relative to the projectile body, which would result in the rear deformation. The axle of the motor in launch 36 was not pushed rearward, as the axle had in launch 5. This is likely due to the cutting down of the axle in launch 36 to shorten its length, which was not done with the same motor type in Launch 5. Cutting the axle causes the end to deform slightly, giving it an oval shape that cannot fit back through the hole out of which the axle protrudes.

Figure 31: Short IR type motor prior to insertion in rubber well nut for launch number 5

Figure 32: Comparison of unfired (bottom) and fired (top) Short IR type motors indicating compression of shaft into casing by launch loads.

Two launches using Mounting Method A were conducted with Long Silver type motors, launches number 33 and 40. Both were launched axle pointing forward. Launch number

33 modified the motor only by removing the vibration weight and cutting down excess axle length. However, launch 40 removed the forward axle completely. Both the Long Silver and Short Silver motors have a two piece axle attached via a male-female sleeve fitting. The forward axle can be pulled out of the sleeve leaving only the rear portion, which is attached to the windings. Doing so results in a motor in which the windings still rotate, but no external axle is protruding from the casing. Figure 33 shows a motor disassembled in this manner. A motor in this configuration would be of limited actual utility. However, the purpose of several launches was to determine if the axle is what was shifting, or otherwise failing, in the Long Silver motors. In this case removing a portion of the axle is of interest. Neither the motor in launch 33 or 40 operating post launch and recovery. Both projectiles are suspected to have been tumbling prior to entry into the soft capture device. However, as subsequent launches showed, tumbling, while undesirable from the standpoint of controlling deceleration conditions, did not seem to limit the ability of motors to survive the test. The estimated peak launch loads experienced by each are approximately 30,000 and 33,000 g's for launches 33 and 40 respectively. However, the motor in launch 40 saw visible deformation of the rear of the motor as seen in Figure 35 and Figure 36, likely caused by setback loads, while launch 33 did not. The damage seen for launch 40 caused a short circuit when the motor was hooked up to power. In contrast, the failure of the motor in launch 33 resulted in an open circuit without any electrical connection between the positive and negative leads. Subsequent inspection of the Long Silver type motor used in launch 33 showed that the axle was seized. However, when the rear contacts assembly was removed the axle turned freely. The inner contacts appeared to be intact. The failure is therefore due to the axle

and windings assembly traveling rearward due to the shock and binding up in some

manner with the rear contacts assembly. Section 4.7 discusses the anatomy of the motors

in more detail.

Figure 33: Disassembly of Long Silver motors with axle intact (left) and fore/aft section separated (right)
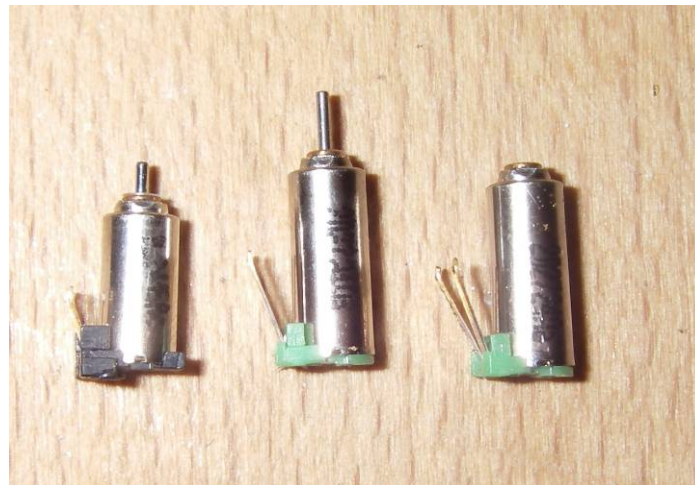
Figure 34: Motor types from left to right; Short Silver, Long Silver, and Long Silver with forward

axle removed

Figure 35: Long Silver type motor with rear end deformed due to setback loads in launch 40
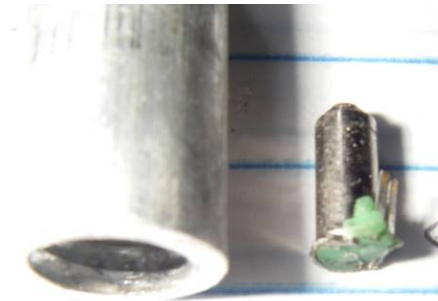
Figure 36: Long Silver type motor with rear end deformed due to setback loads in launch 40

Three launches using Mounting Method A with Short Silver type motors and a standard powder load were conducted. Launches 17, 32 and 34 experienced approximately 33,000, 33,000, and 29,000 g's peak launch acceleration respectively. These launches saw similar deceleration distances in the soft capture device, which would be expected based on the close launch velocities. Figure 37 shows a disassembled view of a short silver motor. For all launches, the offset weight and rubber casing, if present, were removed. This left essentially three components for each motor, the casing including axle bearing, axle and windings assembly, and rear contacts assembly.

Launch 17 used a small amount of wax as a seal between the rear of the motor and the set screw, while the other launches did not. The motor used in launch 17 was inoperable after recovery and it was observed upon disassembly that the wax, although in solid form, had flowed as a result of the acceleration, possibly weakened by the momentary spike in temperature, into the rear portion of the motor housing resulting in an open circuit between the leads. Launches 32 and 34 did not use wax to seal the rear portion of the motor. Launch 32 was launched axle forward and launch 34 axle pointing rearward. Both of these launches resulted in functioning motors after recovery. However, both motors sounded audibly higher pitched when operating than they did pre-launch. These launches

showed that with a simple encapsulation type mounting method around the body of the

motor, with the axle un-encapsulated and free to rotate, that the Short Silver type motor

could survive launch loads in the neighborhood of 30,000 g's.

Figure 37:   Components of Small Black Pager motor type from left to right; rubber casing, rear contact assembly, axle/winding assembly, case, and vibration weight

4.6.3 Mounting Method B

A total of 19 launches were conducted using Mounting Method B, described in Section

3.4.2, which involves using candle wax as an encapsulant to encase the entire motor

including axle. As opposed to Method A, Method B does not allow the axle of the motor

to sit in free space in an orientation where it could potentially operate in flight. However,

this configuration is still interesting for testing, as it would indicate if a fully encapsulated

motor could survive. If so the configuration could then potentially be modified to allow

free rotation of the axle. Table 14 and Table 15 describe the launch parameters and

results for those launches using Mounting Method B.

Table 14: Parameters for Mounting Method B launches with Standard Deceleration Materials

#	Projectile	Motor	Modifications	Mounting Method	Est. Peak G	Cardboard	Sheetrock	Stabilty
					G's	inches	inches	
8	Al Long #1	#29 - LoSi	None	Method B: Axle Forward	11000	13.5	NA	Tumbling
9	Al Long #2	#43 - LoIR	None	Method B: Axle Forward	11405	11	NA	Tumbling
10	Al Short #1	#20 - ShSi	Weight, rubber case removed	Method B: Axle Forward	31734	22	NA	Tumbling
11	Al Long #3	#11 - LaBl	Weight removed	Method B: Axle Forward	8488	21	NA	Tumbling
12	Br Long #1	#30 - LoSi	None	Method B: Axle Rearward	139	NA	5.6	Tumbling
13	Br Long #2	#46 - LoIR	None	Method B: Axle Rearward	143	NA	6.9	Tumbling
14	Al Short #2	#22 - ShSi	Weight, rubber case removed	Method B: Axle Rearward	39166	28.5	NA	Tumbling
15	Br Long #3	#14 - LaBl	Weight removed	Method B: Axle Rearward	140	NA	6.9	Tumbling
16	Al Short #1	#20 - ShSi	Weight, rubber case removed	Method B: Axle Forward	40000	23	NA	Tumbling
18	Al Short #3	#32 - LoSi	Weight removed	Method B: Axle Forward	33000	29	NA	Unclear
19	Al b2 #1	#24 - ShSi	Weight, rubber case removed	Method B: Axle Forward	42121	28	NA	Stable
20	Al b2 #2	#41 - ShSi	Weight removed	Method B: Axle Rearward	23000	20	NA	Unclear
21	Al b2 #3	#23 - ShSi	Weight, case removed / Rear plastic, leads, axle cut	Method B: Axle Forward	46135	26	NA	Stable
23	Al b2 #5	#9 - LoSi	Weight, forward axle removed	Method B: Axle Forward	27000	41	NA	Stable
24	Br Short #2	#10 - LoSi	Weight, forward axle removed	Method B: Axle Forward	20000	30	8.1*	Stable
25	Al Long #1	#42 - ShSi	Weight removed	Method B: Axle Forward	11000	23	NA	Tumbling
29	Al Short #1	#51 - ShSi	Weight, rubber case removed / JB weld encasement	Method B: Axle Forward	40015	23	NA	Tumbling
30	Al b2 #1	#76 - LoSi	Weight, case, forward axle removed / JB weld encasement	Method B: Axle Forward	57479	30.5	NA	Stable
31	Al b2 #2	#87 - LoSi	Weight, forward axle removed	Method B: Axle Rearward	22844	22	NA	Unclear

Table 15: Results for Mounting Method B launches

Launch	Component	Operates	Visible Damage	Voltage	Current
				V	A
8	#29 - LoSi	Partial Turn Only	None	3.7	0.06
9	#43 - LoIR	No	None	3.7	0.03
10	#20 - ShSi	Yes	None	3.7	0.07
11	#11 - LaBl	No	None	3.7	0
12	#30 - LoSi	No	Weight and axle bent	3.7	0
13	#46 - LoIR	No	Rear of motor caved in	3.7	0
14	#22 - ShSi	No	None	3.7	0
15	#14 - LaBl	No	None	3.7	0
16	#20 - ShSi	No	None	3.7	0
18	#32 - LoSi	No	None	3.7	0
19	#24 - ShSi	No	None	3.7	0
20	#41 - ShSi	No	None	3.7	0
21	#23 - ShSi	No	None	3.7	0
23	#9 - LoSi	No	None	3.7	0
24	#10 - LoSi	No	None	3.7	0
25	#42 - ShSi	No	None	3.7	0
29	#51 - ShSi	No	None / Initially pulls 0.25 A then quickly falls to 0.00	3.7	0
30	#76 - LoSi	No	None	3.7	0.08
31	#87 - LoSi	No	Leads bent	3.7	0

Launches number 12, 13 and 15 used the Long Brass type cargo round. Because of their large surface area which increases friction in the barrel, and their large mass, the Long Brass rounds had very low muzzle velocities. This makes their launch environment, which saw muzzle velocities of only a couple hundred feet per second, not relevant to typical gun launch loads. Furthermore, these very long projectiles are observed to be unstable in flight, tumbling prior to entry into the soft capture device. These launches were all decelerated in sheetrock, and despite the low launch velocities they experienced

violent g-forces forces in the relatively hard sheetrock. As a result the Long Silver type and Long IR type motors tested in this manner, launches 12 and 13, experienced motors with significant structural damage. However, the Large Black type motor launched in this way had no visible damage. But, all motors launched in Long Brass rounds were inoperable upon recovery. The motor from launch 12 was later disassembled and it was found that previously solid wax had flowed into the rear motor cavity as a result of the high-g's.

The removed rear portion of a Long Silver type motor is shown in Figure 38. The wax was found in this portion of the motor blocking the interior contacts. To ensure that the wax was indeed entering the casing as a result of the launch environment, rather than during the potting process itself, motor #8, a Long Silver type motor, was mounted in still hot liquid wax. The wax was then allowed to harden then the motor was dug out, without having been launched, and the motor was shown to operate.

Figure 38: Removed rear portion of Long Silver type motor

Neglecting the launches using low velocity Long Brass cargo rounds, there was one launch each using the Long IR and Large Black motor types with Mounting Method B. Launch number 9 used a Long IR motor in an axle forward configuration and experienced approximately 11,000 peak launch g's. Despite the relatively low g's this motor did not operate post recovery. This type of motor however does not have the rear

hole that most other types do, so it is unlikely that failure occurred due to flow of wax into the motor casing.   Unfortunately the construction of the Short and Long IR type motors is such that disassembling and inspection is problematic without damaging the motor. Launch 11 used a Large Black type motor in a similarly moderate-g launch as launch 9. Similarly, this motor did not survive.

Again neglecting launches with Long Brass type projectiles, six Mounting Method B launches were conducted with Long Silver type motors. Of these only one motor, launch 8, was able to turn partially after recovery. When hooked up to power the axle turned approximately ¼ turn then stopped. It would do so again if power was removed and reconnected. Launch 8 was the only launch that used a Long Silver type motor, and partially operated after recovery. This could have been due to the relatively low g's of the launch at only approximately 11,000, compared to the 20,000 to 57,000 approximate peak g's of the other Long Silver motor launches using Mounting Method B. The method of failure for most other Long Silver type motors using wax encapsulation was flow of wax into the rear of the motor casing. It is therefore believed that somewhere between 11,000 and 20,000 g's is necessary for the solid wax to be forced through the small opening in the rear of these motors.

Launches 18, 23, 24, 30 and 31 also launched wax encapsulated Long Silver type motors, none of which operated post recovery. As with all other launches the rubber outer motor casings and vibration weights were removed from these motors before testing. However, in some cases further mass was removed by clipping the leads, axle, and the plastic rear of the motor. For launch 30, the two part epoxy JB Weld was used to encase the rear of the motor in a hard substance that would not flow under high-gs' as the wax had been

demonstrated to do. An example of JB Weld sealant can be seen in Figure 39. Launch 30, however, achieved the highest measured muzzle velocity, 2584 ft/s, of any launch. The non linear relationship between launch velocity and estimated peak acceleration resulted in peak launch loads in the range of 57,000 g's for this launch. Most other peak accelerations for launches were in the 30,000 g range. The motor in launch number 30 had no visible exterior damage; however, it was not operable post recovery. In further testing it would be desirable to launch additional long silver type motors in more moderate-g launches with JB Weld sealant of the aft section.

Eight total Mounting Method B launches were conducted with Short Silver motors. As the smallest available motor, and among the cheapest, the Short Silver motors were the most desirable to g-harden. Launch 29 used a motor with JB weld encased rear portion, as shown in Figure 39. This launch saw a relatively high peak acceleration, compared to other launches, of 40,000 g's, and the motor was not operable post launch. Assuming that when the rear of the motor was sealed, encasement in wax was at least as effective as in a rubber well nut, would mean that the failure point of the Short Silver motors with this type of modification, and when encapsulated, is between 33,000 to 40,000 g's. Launches 10, 14, 16, 19, 20, 21, and 25 launched Short Silver motors encased in wax in both axle forward and rearward orientations, and with varying levels of mass reduction. However, none of these launches used any barrier to prevent wax from flowing into the motor casing. The motor in launch 10 survived and operated post launch. This motor was subsequently launched again in launch 16, where it did not operate post recovery. Upon disassembling it was seen that wax had entered the rear of the motor casing. The peak acceleration for launch number 10 was 32,000 g's, compared to an estimated 40,000

for launch 16. The failure could have been due to the increased g's of the second launch, however more experiments would be required before being confident of this explanation. None of the other Short Silver type motors survived using wax encapsulation. The motor in launch 19 was disassembled and it was verified that wax flow was responsible for the failure.

Figure 39: Short Silver type motor, launch 29, with JB weld sealed rear portion (right) versus original condition (left)

4.6.4 Mounting Method C

Two launches were made using Mounting Method C, a non-encapsulated compression mount, as described in Section 3.4.3. However, only one of the two projectiles was recovered. The recovered round was from launch 35, which used the very stable Brass b2 cargo round, and launched the payload at approximately 24,000 g's peak acceleration. The launch parameters and results for this launches are summarized in Table 16 and Table 17. As with almost all other launches, the rubber case and vibration weight were removed from the motor. The axle was also cut down to reduce mass. The Short Silver type motor was mounted axle forward with the axle sticking through the holes in a stack of washers in the fore end of the projectile cavity, and the rear of the motor firmly compressed by the set screw. The damage incurred by the motor is shown in Figure 40 and Figure 41. The rear of the motor was severely damaged, with the casing and

windings being crushed inwards. However, the front of the motor appears intact. Upon recovery the motor was loose in the cavity of the projectile, no longer being pressed down by the set screw. This is believed to have resulted from the shortening of the motor under the crushing acceleration force upon launch. This launch demonstrated the necessity of encapsulating the motor. Without encapsulation around the motor casing the empty space serves as volume that the motor structure can deform into under the extreme loads associated with gun launch.

Table 16: Parameters for Mounting Method C launch

#	Projectile	Motor	Modifications	Mounting Method	Est. Peak G	Cardboard	Sheetrock	Stabilty
					G's	inches	inches	
35	Br b2 #1	#55 - ShSi	Weight, rubber case removed / Axle cut	Method C: Axle For., 8 washers	24181	37.5	NA	Stable

Table 17: Results for Mounting Method C launch

Launch	Component	Operates	Visible Damage	Voltage	Current
				V	A
35	#55 - ShSi	No	Washers undamaged, rear of motor deformed inwards, front appears intact, motor loose in bullet	3.7	Max (3.04)

Figure 40: Short Silver type motor after launch before being extracted from cargo round, launch 35

Figure 41: Short Silver type motor showing damaged rear portion and broken off plastic piece in foreground, launch 35

4.6.5 Ultra High-G Deceleration

In order to investigate the effects of g-loads significantly higher than the 30,000 average

peak launch loads experienced in the standard test launches, the deceleration event was

used to shock two motors to much higher levels. For these tests, light Aluminum b2 type

cargo rounds were used to launch Short Silver type motors. The peak acceleration for the

launches was approximately 29,000 and 27,000 g's for launches 22 and 39 respectively.

However, by using sheetrock instead of cardboard it was possible to decelerate them in

less than 5 inches as opposed to the 20 to 35 inches it would have taken in cardboard.

Using constant acceleration as an approximation, and the measured deceleration distances

in sheetrock gives a deceleration g-load of 172,000 and 160,000 g's for launches 22 and

39. As would be expected under such extreme loads, neither motor remained structurally

intact or operable. In the case of launch 22, which used an unstable round that tumbled

before decelerating, the axle was bent and jammed backwards into the case. In the case

of launch 39, where the round was observed to be stable, the axle and windings came

forward out of the casing as would be expected with a violent deceleration in the opposite

direction, this damage can be seen in Figure 42 and Figure 43. These two ultra high-g

deceleration launches demonstrate that even with optimal encapsulation techniques these

types of motors would be unlikely to survive loads in this range.

Table 18: Parameters for Ultra High-G Deceleration launches

#	Projectile	Motor	Modifications	Mounting Method	Est. Peak G	Cardboard	Sheetrock	Stabilty
					G's	inches	inches	
22	Al b2 #4	#25 - ShSi	Weight removed	Method B: Axle Forward	*29000*	NA	4.4	Tumbling
39	Al b2 #5	#57 - ShSi	Weight, rubber case removed / Axle cut	Method A: Axle Forward	27000	NA	4.4	Stable

Table 19: Results for Ultra High-G launches

Launch	Component	Operates	Visible Damage	Voltage	Current
				V	A
22	#25 - ShSi	No	Axle bent and jammed into case	3.7	0
39	#57 - ShSi	No	Al. bullet splinters behind motor, part of plastic rear broke off, windings and axle ejected forward	3.7	Max (3.04)
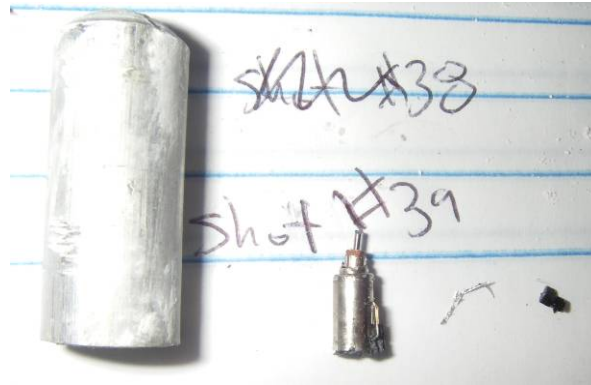
Figure 42: Launch 39 result showing axle and windings ejected from casing

Figure 43: Launch 39 result showing ejection of axle and windings due to violent deceleration

4.6.6 Low-G Launches

Two launches, number 37 and 38, were performed with ½ of the powder load as all other launches. This was done in order to see the effect of a relatively low-g launch. Based on their measured muzzle velocities the estimated peak g's for launches 37 and 38 are 7,000 and 10,000 respectively. Launch 37 used a Short Silver type motor with similar modifications and the same mounting method as with launch 32. Launch 32, which used a full powder load, had significantly higher g's at 33,000 and survived. It was therefore expected that the motor in launch 37 would also survive. However, the recovered motor was not operable, pulling 0.25A but not turning. Inspection revealed that the axle was seized. Upon disassembly, it was shown that when the rear contacts assembly was

removed the axle would turn freely again. No visible damage was seen inside the motor casing. The only difference between the launches was the cargo round used and the cutting of the axle to shorten it in launch 37. It is unlikely that the cargo round is the cause of the failure, as the cargo round in launch 32 was much more stable than the round in launch 37. The only remaining explanation therefore is the cutting down of the axle. This should make the axle lighter and therefore more apt to survive. However, as mentioned previously, when cutting the end off the base of the axle that sticks out from the casing is slightly flattened. If the axle traveled backwards under acceleration loads and was not cut, it would go back into the case and then perhaps recover as a result of setforward loads when exiting the muzzle, or upon deceleration in the soft capture device. However, if the cut axle can't travel back into the case it might be pushed back just far enough to be wedged in the bearing at the forward end of the case. For future experiments, it would be desirable to conduct several otherwise identical launches with axle cut and unmodified axle motors to determine if this is a cause of failure.

Launch 38 used a Long Silver type motor which resulted in a deformed rear end despite the relatively low g's, see Figure 44. The fact that this motor was inoperable was not surprising based on similar launches at higher g's. However, the degree of damage to the rear of the motor indicates this launch too might have experienced problems with the mounting of the motor.

Table 20: Parameters for Low-G, reduced powder, launches

#	Projectile	Motor	Modifications	Mounting Method	Est. Peak G	Cardboard	Sheetrock	Stabilty
					G's	inches	inches	
37	Br b2 #3	#56 - ShSi	Weight, rubber case removed / Axle cut	Method A: Axle Forward	6522	23	NA	Stable
38	Br b2 #4	#88 - LoSi	Weight removed / Axle cut	Method A: Axle Forward	10247	39	NA	Stable

Table 21: Results for Low-G, reduced powder, launches

Launch	Component	Operates	Visible Damage	Voltage	Current
				V	A
37	#56 - ShSi	No	None	3.7	0.25
38	#88 - LoSi	No	Rear of plastic and motor deformed inwards	3.7	Max (3.04)

Figure 44: Damage to motor rear end resulting from launch 38

4.7 Loads Analysis

In order to better understand the acceleration loads involved, a very simple structural analysis was conducted of the Short Silver type motor in two configurations. Wilkerson [21] describes the conventional method of analyzing launch loads in projectiles as a "quasi-static, axisymmetric, finite-element approach that balances the peak propellant pressure on the base of the projectile with an equivalent acceleration". The analysis done here is treated as quasi-static and the motor is axisymetric. A quasi-static analysis is adequate as the loading is of relatively low frequency compared to the natural frequencies of the motor sub-components [21]. Instead of a finite element approach, the motor model is split at several cross sections and simple application of Newton's second law used to determine the stresses involved. The equivalent of the pressure on the base of the projectile is the pressure imparted on the rear of the motor by the cargo round, which serves to balance out the acceleration pressure. Not considered in this analysis were balloting, setforward, or rotational loads.

The Short Silver type motor was chosen for analysis as it was the most robust of the tested motors, and the only one to emerge fully functional from any launch. Figure 45

shows a cutaway diagram of the subcomponents of this motor. To aid in reading the

diagram, pictures of the components themselves are shown in Figure 46 and Figure 47.

The measured dimensions and masses of each component are shown in Table 22.
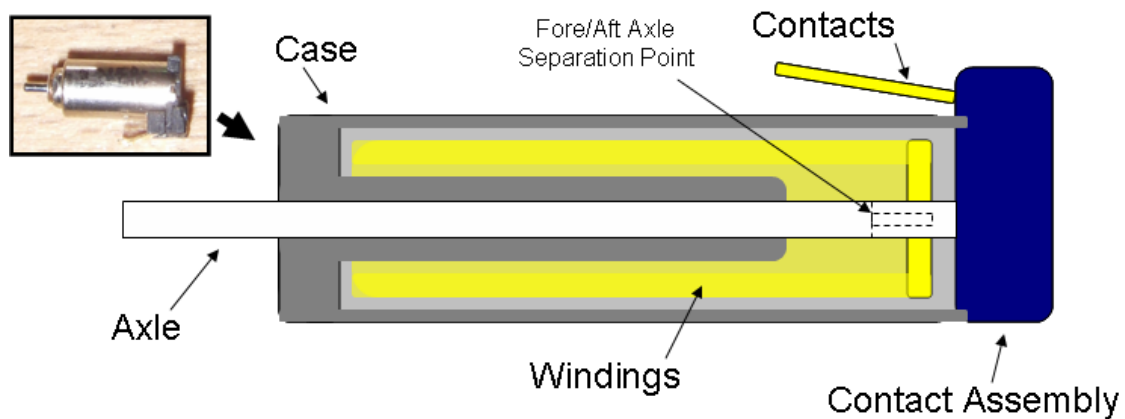
Figure 45: Cutaway diagram of Short Silver type motor

Figure 46: Components of Short Silver type motor from left to right; rear contact assembly, axle/winding assembly, and case

Figure 47: End view of components of Short Silver type motor

Table 22: Short Silver type motor sub-component dimensions and masses

Measurement	mm
Case Diameter	4.0
Case Length	10.7
Case Thickness	0.3
Contact Assembly Height	5.4
Contact Assembly Width	4.6
Contact Assembly Thickness	1.6
Axle Length	10.6
Axle Diameter	0.7
Windings Diameter	3.1
Windings Length	5.2
Windings Thickness	0.2
Sub-component	**grams**
Case	0.32
Contact Assembly	0.06
Windings	0.03
Rearward Axle and Winding Cap	0.01
Forward Axle	0.02
Total Mass	0.44

The two cases analyzed here are representative of launches 32 and 34, which resulted in functioning motors. Both were encapsulated in a rubber well nut using Mounting Method A. Launch 32 was configured axle pointing forward, and Launch 34 axle rearward. The launch loads based on the measured muzzle velocities for each were 33,000 and 29,000 g's, for Launches 32 and 34 respectively. Figure 48 and Figure 49 show diagrams of the configurations, indicating direction of acceleration and the points at which stress is analyzed. The points, labeled 1 through 7 on the two diagrams, were selected to be areas where the greatest stress would be concentrated based on the direction of acceleration and the structure of the motor.
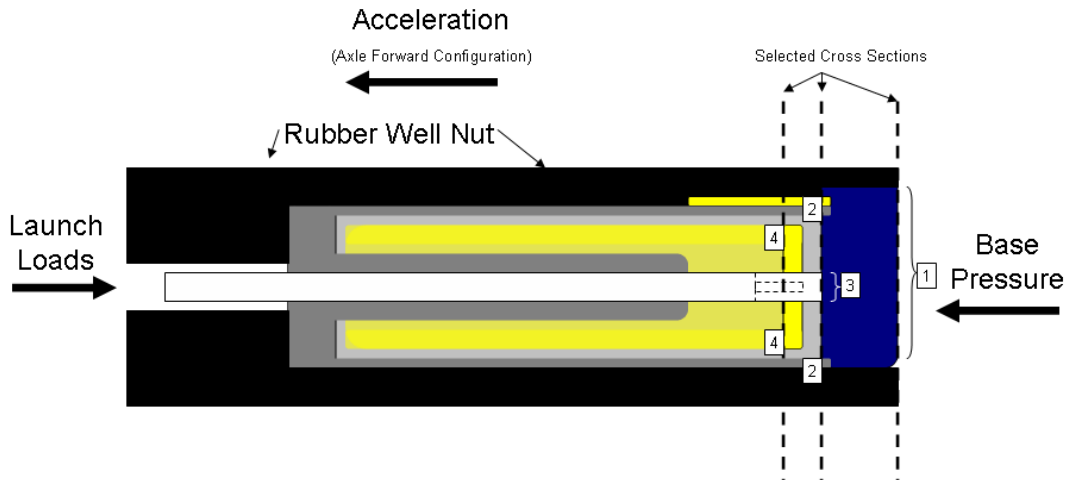
Figure 48: Axle forward configuration (Launch 32) showing cross sections for stress analysis (Points 1, 2, 3, and 4)
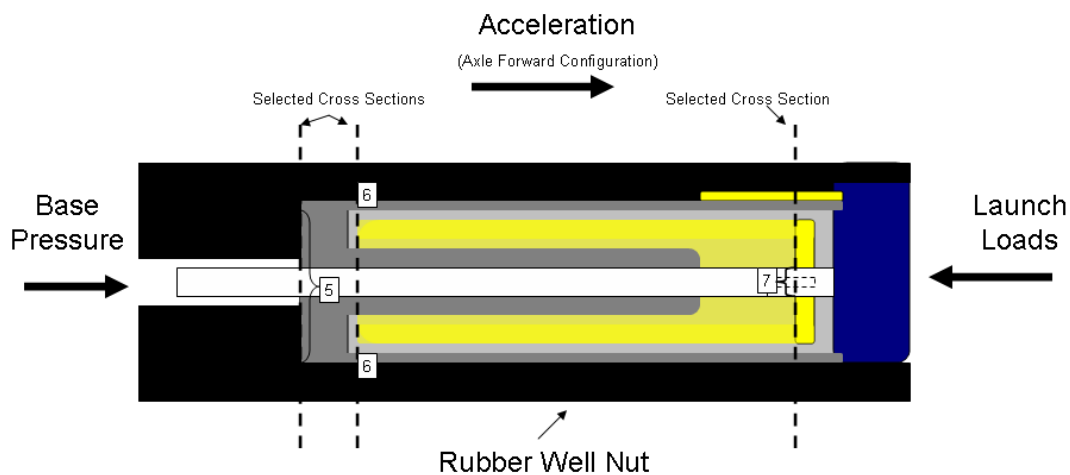
Figure 49: Axle rearward configuration (Launch 34) showing cross sections for stress analysis (Points 5, 6, and 7)

The first two columns in Table 23 identify each of the seven points of stress analysis for the configurations shown in Figure 48 and Figure 49. Since the analysis is axisymmetric, the next step was to determine the relevant cross sectional area of each area of interest based on the measurements shown in Table 22. The *Loading Elements* column in Table 23 describes the sub-components of the motor that are causing load to be applied at each point when under acceleration. The mass of these loading elements is then tabulated in the *Mass* column. Finally the average force over each cross section and the stress in that section are calculated using the following simple relationships:

$$F = m \times A_{launch} \tag{5}$$

$$\sigma = \frac{F}{A} \tag{6}$$

Table 23: Loads analysis points, relevant cross sectional area, and calculated stress

Point	Description	Area	Loading Elements	Mass	Force	Stress
		mm^2		g	N	N/mm^2
Launch 32, Axle Forward, Mounting Method A, Short Silver type motor, 33,000 g's						
1	Base of Contact Assembly	24.7	Entire motor	0.44	142.2	5.8
2	Case Cross Section	3.4	Case	0.32	103.4	30.3
3	Axle Cross Section	0.4	Forward/Rearward Axle and Windings	0.06	19.4	51.8
4	Windings Cross Section	1.6	Windings	0.03	9.7	5.9
Launch 34, Axle Rearward, Mounting Method A, Short Silver type motor, 29,000 g's						
5	Case Contact With Well Nut	12.4	Entire Motor	0.44	125.9	10.1
6	Case Cross Section	3.4	Contact Assembly and Case Barrel Section*	0.14	40.1	11.7
7	Axle Attachment to Windings	0.4	Forward/Rearward Axle and Windings	0.06	17.2	45.9

*Mass of barrel section of case could not be measure independently and is estimated here to be 0.08g

For the axle forward configuration, the highest calculated stress, as shown in Table 23, was at point 3. This is at the rear of the axle where the mass of the axle and windings, which is relatively low never-the-less causes a high stress point, 51.8 N/mm^{2}, because of the small cross section of the axle. It is not believed that the solid aluminum rod of the axle would fail, however the force could tend to cause the axle to travel backwards and damage the contacts assembly. This type of damage was seen in several launches. The stress in the rear of the case cross section, point 2, is also relatively high at 30.3 N/mm^{2}. This is another potential failure point, and in fact was seen in several other launches where the rear of the case was deformed against the cargo round set screw. The loads at points 1 and 4 were moderate by comparison. Based on observed results it is believed that the previously described two modes of failure would occur before failure at points 1 or 4.

For the axle rearward configuration, the highest calculated stress was at point 7, 45.9 N/mm^{2}. At this point the mass of the axle and windings is pulling under load. Again,

because of the solid construction of the axle and based on observation it is not believed that the axle itself would fail under these loads. However, this could cause the axle to travel rearward. In the case of axle rearward mounting this would not cause the axle to impact the contact assembly. But if it traveled too far forward could cause it to separate from the contact assembly. Points 5 and 6 had more moderate calculated stresses and are believed to be secondary to concerns with the axle with respect to failure modes.

4.8 Specific Example Applications

This project has demonstrated the g-hardening of a very low cost COTS DC electric motor to gun launch loads on the order of 30,000 g's. G-hardening to this level would allow survival of gun launch loads in many large caliber rounds, such as most 155mm artillery rounds. However, the launch loads seen by smaller caliber rounds such as the .50 BMG are higher, sometimes reaching as high as 65,000 g's.

Although the g-hardening of motors for this project fell short of 65,000 g's, the results point strongly to the feasibility of g-hardening small electric motors for small caliber systems. A combination of further work to extend the limit of survivability for the motor, accepting slightly lower muzzle velocities, and use of slow burning powders, could allow these motors to survive loads in small caliber projectiles such as .50 rounds. Applications within guided small or large caliber systems where these motors might prove useful include mechanical actuators for control devices, electrical generators using ram air, or as a mid course stability effecter.

As mechanical actuators these types of small DC motors could be paired with aerodynamic control surfaces, valves controlling ram air flow paths, or other devices to effectively control a guided projectile in flight. Obviously, much work would be required

to adapt the motors used here to the desired system. However, this project shows the feasibility of using such motors in high-g applications.

With any military ammunition, guided or unguided, it is highly desirable for the system to have a shelf life that is many years with no maintenance required. With standard dumb rounds, this is relatively easy to achieve. However, with guided projectiles this presents a potential challenge with the power source. Batteries have been demonstrated to withstand high-g environments. However they will eventually degrade when stored for long periods of time. A small electric motor could be used as a ram air powered electrical generator. This would essentially bleed off forward velocity to produce electrical power for the projectile's systems. The additional drag would decrease the range of the projectile, for a mathematical discussion of exterior ballistics and drag refer to Klimi [14].

The vast majority of small caliber projectiles are spin stabilized. Spin stabilization keeps the projectile from excessive yawing, or even worse, tumbling. This increases the range and accuracy versus an unstable round. However, in terms of terminal ballistics, ballistics after impacting the target, projectile instability can be a desirable trait. As described by Fackler [9], an unstable round can have significantly increased lethality. If desired, a small electric motor could be used to shift an internal mass inside a projectile during mid-flight, inducing instability. This would allow for a stable round during the majority of the flight followed by a destabilization of the round just prior to impacting the target.

CHAPTER 5

5 Conclusion

This project has demonstrated the g-hardening of very small COTS DC electric motors to a level necessary to survive gun launch loads. Different methods of managing the load path were explored including encapsulation, mounting orientation, mass reduction and pre-loading. A series of experiments in which motors were mounted inside of cargo rounds, launched in live fire tests and subsequently recovered resulted in demonstration of survivability of one type of motor to peak setback loads of greater than 30,000 g's. The motor also survived the associated setforward and balloting loads typical of a gun launch environment. Analysis of the different mounting methods, motor modifications, motor types, and test conditions for 31 launches with recovered motors was conducted to determine the causes of the failure or success.

These motors are extremely small, with the modified motors of the final successful launches being less than 11.4 mm in length and 5.4 mm at their widest point, with a mass of 0.43 grams. They are also low cost, as they are mass produced for use as vibration motors in cell phones and pagers. Purchased in single quantities these motors can be obtained for as little as $0.62 per motor. These traits make these g-hardened motors suitable candidates for use in the next generation of small caliber guided projectiles which may benefit from small and very low cost electromechanical devices. Several potential applications for small caliber guided projectiles have been identified including actuators for control mechanisms, electrical generators, and mid-course stability effectors. Further work would be required to make these motors suitable for particular

applications, however this project has experimentally demonstrated that an affordable miniature electric motor can be mounted in a projectile, launched, and survive gun launch loads in order to be used during flight.

Bibliography

[1] Berman, Morris S., Electronic Components for High-g Hardened Packaging.
Technical Report Army Research Laboratory ARL-TR-3705, 2006.

[2] Combs, S. K., Foust, C. R., Gouge, M. J., Milora, S. L., Acceleration of Small, Light
Projectiles (Including Hydrogen Isotopes) to High Speeds Using a Two-Stage Light
Gas Gun. Oakridge National Laboratories. CONF-891093—9, DE90 002479.

[3] Connecticut Valley Arms, Conventional and Bolt Action In-Line Rifles. Form 103
Ref 01/01. Connecticut Valley Arms 2001.

[4] D'Amico, William. Revolutionary Technologies for Miniature Measurement Systems
– Applications to Ground Testing. AIAA A98-16141. 36th Aerospace Sciences
Meeting & Exhibit. 12-15 January 1998. Reno, Nevada.

[5] D'Amico, William P., Telemetry Systems and Electric Gun Projectiles. Technical
Report Army Research Laboratory ARL-MR-499, 2000.

[6] Davis, Bradford S., Flight test results of miniature, low cost, spin, accelerometer, and
yaw sensors. AIAA Paper 97-0422, 1997.

[7] Davis, Bradford S., Hepner, David J., Hamilton, Michael B., Shock Experiment
Results of the DFuze 8-Channel Inertial Sensor Suite That Contains Commercial
Magnetometers and Accelerometers. Technical Report Army Research Laboratory
ARL-MR-532, 2002.

[8] Edwards, John A., Concepts Behind the UK HOTLiP Maneuvering Projectile
Program. AIAA 2001-4317. AIAA Atmospheric Flight Mechanics Conference &
Exhibit. 6-9 August 2001. Montreal, Canada.

[9] Fackler, Martin L., Surinchak, John S., Malinowski, John A., Bowen, Robert E., Wounding Potential of the Russian AK-74 Assault Rifle. The Journal of Trauma 0022-5282/84/2403-0263$02.00/0. Vol. 24, No. 3. 1984.

[10]   Fiske, James O., Ricci, Michael R., Ricce, Kenneth, Hull, John R., The Launch Ring – Circular EM Accelerators for Low Cost Orbital Launch. AIAA 2006-7279. Space 2006. 19-21 September 2006. San Jose, California.

[11]   Gonzalez, Joe R., Interior Ballistics Optimization. Master Thesis AD-A225 791. Dept. of Mechanical Engineering. Kansas State University. 5 June 1990.

[12]   Kessler, Seth S., Spearing, Mark S., Kirkos, Gregory A. Design of a High-g Unmanned Aerial Vehicle Structure. AIAA 2000-01-5538. 2000 World Aviation Conference. 10-12 October 2000. San Diego, California.

[13]   Killen, Albert. Tarrant, David. Jordan, Robert. Becka, Stephen. Improved High Acceleration, High Performance Solid State Accelerometer. AIAA-95-3235-CP. 1995.

[14]   Klimi, Gjergj, Exterior Ballistics of Small Arms, Xlibris Corporation. 2009.

[15]   Martorana, Richard T., WASP—A High-g Survivable UAV. AIAA-2002-3439. AIAA 1st Technical Conference and Workshop on Unmanned Aerospace Vehicles. 20-23 May 2002. Portsmouth, Virginia.

[16]   Massey, K. C., McMichael J., Warnock T., Hay F., Mechanical Actuators for Guidance of a Supersonic Projectile. AIAA 2005-4970. 23rd AIAA Applied Aerodynamics Conference. 6-9 June 2005. Toronto, Ontario, Canada.

[17]   Quesenberry, Matthew J., Madison, Phillip H., Jensen, Robert E., Characterization of Low Density Glass Filled Epoxies. Technical Report Army Research Laboratory ARL-TR-2938, 2003.

[18]   Rinker, Robert A., Understanding Firearm Ballistics, Sixth Edition. Mulberry House Publishing. 2010.

[19]   Shaver, Joel E., Jones, Gil R., Walker, Greg P., Application of Gun-Launched Telemetry at the AEDC Range G Facility. AIAA 96-4508. AIAA 7th International Aerospace Plane and Hypersonic Technologies Conference. 18-22 November 1996. Norfolk, Virginia.

[20]   Shaver, J. E., Walker, G. P., Russell S.M., Hardened Subminiature Telemetry at the AEDC. AIAA 95-3989. 1st AIAA Aircraft Engineering, Technology, and Operation Congress. 19-21 September 1995. Los Angeles, California.

[21]   Wilkerson, Stephen. Hopkins, David. Gazonos, George. Berman, Morris. Developing a Transient Finite Element Model to Simulate the Launch Environment of the 155-mm SADARM Projectile. Technical Report Army Research Laboratory ARL-TR-2341, 2000.

Appendix A

Appendix A: Component Test #3 Yaw Card Results

Figure 50: Yaw card for launch 29 with Short Al #1 cargo round

Figure 51: Yaw card for launch 30 with Short Al b2 #1 cargo round

Figure 52: Yaw card for launch 31 with Short Al b2 #2 cargo round

Figure 53: Yaw card for launch 32 with Short Al #2 cargo round

Figure 54: Yaw card for launch 33 with Short Al b2 #3 cargo round

Figure 55: Yaw card for launch 34 with Short Al b2 #4 cargo round

Figure 56: Yaw card for launch 35 with Short Br b2 #1 cargo round

Figure 57: Yaw card for launch 36 with Short Br b2 #2 cargo round

Figure 58: Yaw card for launch 37 with Short Br b2 #3 cargo round

Figure 59: Yaw card for launch 38 with Short Br b2 #4 cargo round

Figure 60: Yaw card for launch 39 with Short Al b2 #5 cargo round

Figure 61: Yaw card for launch 40 with Short Al #3 cargo round

Appendix B

Appendix B: Physical and Cost Information for Motors Prior to Modification

Table 24: Physical and cost information for motors prior to any modification

#	Type	Lot / Casing	Voltage	Current	Length	Width	Mass	Unit Cost
-	-	-	V	A	mm	mm	G	-
1	IR Heli	IR Heli	3.7	0.01	12	4.07	0.49	$11.95
2	IR Heli	IR Heli	NA	NA	NA	NA	NA	$11.95
3	Long Silver	Blue Case	3.7	0.06	16.35	5.82	1.36	$0.62
4	Long Silver	Blue Case						$0.62
5	Long Silver	Blue Case						$0.62
6	Long Silver	Blue Case						$0.62
7	Long Silver	Blue Case	3.7	0.07	16.26	5.94	1.35	$0.62
8	Long Silver	Blue Case						$0.62
9	Long Silver	Blue Case						$0.62
10	Long Silver	Blue Case						$0.62
11	Large Black	Large Black Pager	3.7	0.27	17.11	5.77	1.71	$0.62
12	Large Black	Large Black Pager						$0.62
13	Large Black	Large Black Pager						$0.62
14	Large Black	Large Black Pager						$0.62
15	Large Black	Large Black Pager	3.7	0.28	17.18	5.78	1.72	$0.62
16	Large Black	Large Black Pager						$0.62
17	Large Black	Large Black Pager						$0.62
18	Large Black	Large Black Pager						$0.62
19	Short Silver	Small Black Pager	3.7	0.22	12.64	5.81	0.97	$0.62
20	Short Silver	Small Black Pager	3.7	0.24	12.56	5.8	0.97	$0.62
21	Short Silver	Small Black Pager						$0.62
22	Short Silver	Small Black Pager						$0.62
23	Short Silver	Small Black Pager						$0.62
24	Short Silver	Small Black Pager						$0.62
25	Short Silver	Small Black Pager						$0.62
26	Short Silver	Small Black Pager						$0.62
27	Long Silver	Long Silver Pager	3.7	0.06	16.46	5.18	1.18	$0.62
28	Long Silver	Long Silver Pager						$0.62
29	Long Silver	Long Silver Pager						$0.62
30	Long Silver	Long Silver Pager						$0.62
31	Long Silver	Long Silver Pager	3.7	0.07	16.35	5.08	1.20	$0.62
32	Long Silver	Long Silver Pager						$0.62
33	Long Silver	Long Silver Pager						$0.62
34	Long Silver	Long Silver Pager						$0.62
35	Short Silver	Short Silver Pager	3.7	0.22	12.41	5.33	0.86	$0.62

#	Type	Lot / Casing	Voltage	Current	Length	Width	Mass	Unit Cost
36	Short Silver	Short Silver Pager						$0.62
37	Short Silver	Short Silver Pager						$0.62
38	Short Silver	Short Silver Pager						$0.62
39	Short Silver	Short Silver Pager						$0.62
40	Short Silver	Short Silver Pager						$0.62
41	Short Silver	Short Silver Pager						$0.62
42	Short Silver	Short Silver Pager						$0.62
43	TPM2	TPM2	3.7	0.02	16.94	4.1	0.66	$5.27
44	TPM2	TPM2						$5.27
45	TPM2	TPM2						$5.27
46	TPM2	TPM2						$5.27
47	TPM2	TPM2	3.7	0.03	16.96	4.08	0.67	$5.27
48	TPM2	TPM2						$5.27
49	TPM2	TPM2						$5.27
50	TPM2	TPM2						$5.27
51	Short Silver	o2 Small Black	3.7	0.23	12.58	5.39	0.98	$1.18
52	Short Silver	o2 Small Black	3.7	0.22	12.56	5.79	0.96	$1.18
53	Short Silver	o2 Small Black	3.7	0.24	12.58	5.81	0.99	$1.18
54	Short Silver	o2 Small Black						$1.18
55	Short Silver	o2 Small Black						$1.18
56	Short Silver	o2 Small Black						$1.18
57	Short Silver	o2 Small Black						$1.18
58	Short Silver	o2 Small Black						$1.18
59	Large Black	o2 Large Black						$1.18
60	Large Black	o2 Large Black						$1.18
61	Large Black	o2 Large Black	3.7	0.30	17.02	5.83	1.66	$1.18
62	Large Black	o2 Large Black						$1.18
63	Large Black	o2 Large Black						$1.18
64	Large Black	o2 Large Black						$1.18
65	Large Black	o2 Large Black	3.7	0.28	17.06	5.75	1.68	$1.18
66	Large Black	o2 Large Black	3.7	0.28	16.93	5.84	1.67	$1.18
67	Braced	o2 Braced						$1.18
68	Braced	o2 Braced						$1.18
69	Braced	o2 Braced	3.7	0.16	16.05	6.52	1.28	$1.18
70	Braced	o2 Braced						$1.18
71	Braced	o2 Braced						$1.18
72	Braced	o2 Braced						$1.18
73	Braced	o2 Braced	3.7	0.16	16.04	6.64	1.30	$1.18
74	Braced	o2 Braced	3.7	0.16	16.03	6.58	1.29	$1.18
75	Long Silver	o2 Blue Case	3.7	0.06	16.31	5.83	1.36	$1.18
76	Long Silver	o2 Blue Case	3.7	0.07	16.33	5.91	1.34	$1.18
77	Long Silver	o2 Blue Case						$1.18
78	Long Silver	o2 Blue Case	3.7	0.07	16.33	5.61	1.34	$1.18
79	Long Silver	o2 Blue Case						$1.18
80	Long Silver	o2 Blue Case						$1.18
81	Long Silver	o2 Blue Case	3.7	0.07	16.31	5.68	1.34	$1.18
82	Long Silver	o2 Blue Case						$1.18

#	Type	Lot / Casing	Voltage	Current	Length	Width	Mass	Unit Cost
83	Long Silver	o2 Long Silver	3.7	0.07	16.48	5.09	1.19	$1.18
84	Long Silver	o2 Long Silver	3.7	0.06	16.3	5.12	1.18	$1.18
85	Long Silver	o2 Long Silver	3.7	0.07	16.19	4.77	1.18	$1.18
86	Long Silver	o2 Long Silver						$1.18
87	Long Silver	o2 Long Silver						$1.18
88	Long Silver	o2 Long Silver						$1.18
89	Long Silver	o2 Long Silver	3.7	0.06	16.25	4.80	1.19	$1.18
90	Long Silver	o2 Long Silver						$1.18

Appendix C

Appendix C: Post-Modification, Pre-Launch Measurements of Motors

Table 25: Post-Modification, Pre-Launch Measurements of Motors

Launch	Component	Voltage	Current	Length	Width	Mass
		V	A	mm	mm	g
5	#2 - ShIR					
8	#29 - LoSi					
9	#43 - LoIR					
10	#20 - ShSi					
11	#11 - LaBl					
12	#30 - LoSi					
13	#46 - LoIR					
14	#22 - ShSi					
15	#14 - LaBl					
16	#20 - ShSi	3.7	0.1	10.91	5.38	0.43
17	#40 - ShSi					0.43
18	#32 - LoSi	3.7	0.02			0.54
19	#24 - ShSi					
20	#41 - ShSi					
21	#23 - ShSi	3.7	0.07			0.38
22	#25 - ShSi					
23	#9 - LoSi	3.7	0.04			0.5
24	#10 - LoSi	3.7	0.05			0.5
25	#42 - ShSi					
29	#51 - ShSi	3.7	0.11	11.36	5.39	0.43
30	#76 - LoSi	3.7	0.05	12.07	5.84	0.52
31	#87 - LoSi	3.7	0.06	11.31	5.27	0.49
32	#53 - ShSi	3.7	0.08	11.33	5.06	0.43
33	#85 - LoSi	3.7	0.03	12.46	5.11	0.52
34	#54 - ShSi	3.7	0.12	11.26	5.36	0.42
35	#55 - ShSi	3.7	0.07	10.39	5.37	0.43
36	#1 - ShIR	3.7	0.02	12.36	4.07	0.44
37	#56 - ShSi	3.7	0.07	11.04	5.34	0.42
38	#88 - LoSi	3.7	0.02	12.57	5.2	0.52
39	#57 - ShSi	3.7	0.08	10.77	5.37	0.43
40	#80 - LoSi	3.7	0.04	11.25	4.95	0.48

Appendix D

Appendix D: Ancillary Experiments

In order to gain a more accessible and intuitive understanding of the magnitude of gun

launch accelerations, a number of side experiments were conducted that have no direct

link to the effort to g-harden small electric motors.

For the first of these launches, a small ant was launched inside of a cargo round, launch 6.

The ant was not encapsulated in any way. Upon recovery, the ant was in the form of a

paper thin dot and unrecognizable as an insect.

Launch 7 launched a popcorn kernel in a long aluminum type cargo round. The muzzle

velocity was not measured but based on similar launches, peak g-loads of only about

10,000 g's would be expected for this round. Despite the relatively low g-loads, the un-

encapsulated popcorn kernel was shattered into many small pieces as can be seen in

Figure 62.

The third side experiment, launch 26, launched a potato bug that was packed in soil.

Upon recovery the potato bug could not be distinguished from the soil.

Figure 62: Side experiment conducted with popcorn kernel, launch 7